2005-01-25

An Analysis of The Effect of 3-D Groove Insert Design on Chip Breaking Chart

Alfred Avanessian
Worcester Polytechnic Institute

An Analysis of The Effect of 3-D Groove Insert Design on Chip Breaking Chart

by

Alfred Avanessian

A Thesis

Submitted to the faculty of

WORCESTER POLYTECHNIC INSTITUTE

in partial fulfillment of the requirements for the

Degree of Master Science

in

Manufacturing Engineering

by

_____

Alfred Avanessian, January 2005

APPROVED:

_____

Yiming (Kevin) Rong, Advisor, Professor of Mechanical Engineering, Associate Director of Manufacturing and Materials Engineering

Abstract

Prediction of chip-breaking in machining is an important task for automated manufacturing. There are chip-breaking limits in machining chip-breaking chart, which determine the chip-breaking range. This thesis presents a study of the effect of 3-D groove insert parameters on chip breaking chart. Based on the chip-breaking criteria, the critical feed rate is formulated through an analysis of up-curl chip formation for 3-D grooves.

Also in order to predict chip-breaking limits, for protruded insert grooves in finish machining, analytical models are established. In the analytical models, minimum and maximum depth of cut are identified for using different chip breaking models. As well insert nose radius effects on chip thickness for small depth of cut are studied. In the end, the analytical critical feed rate model is extended to finish machining with 3-D chip-breaking grooves.

Acknowledgment

This thesis is more than the product of the last couple of years of research and thought. It represents the coming together of many influences over quite a few years and the encouragement of fine friends, family, colleagues, and teachers past and present. I would like to thank the following people:

My advisor, Professor Yiming Rong, for his guidance and support throughout my years at WPI. His critical review of the manuscript, patience and expertise helped me find direction in many areas of research related activities.

I also wish to thank the other committee members, including Professor Richard D. Sisson Jr., Professor Mustafa Fofana and Dr. Hui Song for their useful comments and contributions on improving my writing style.

Professor Christofer A. Brown and Mr. Torbjorn Bergstrom, The Surface Metrology Laboratory Manager, for allowing and helping me to use facilities to take measurements on some inserts.

Dr. William C. S. Weir, Robotics Lab Manager and Mr. Steve Derosier and Todd Billings Haas Technical Education Center Technicians for providing machining facilities.

My two-semester tuition provided by GE and WPI and Mr. Siamak M. Najafi for providing on campus job are also acknowledged.

The members of the CAM Lab at WPI and Mohamed C. Shaw all provided companionship and made fun in addition to providing valuable scholarly input to this work.

Finally, I would like to dedicate this thesis to my parents and siblings for their constant love, moral and financial support during my studies.

Nomenclature

b_{ch}	Chip width (mm), (in)
$b_{\gamma 1}$	Insert/chip restricted contact length (mm), (in)
C_h	Cutting ratio (the ratio of the undeformed chip thickness to the chip thickness)
d	Depth of cut (mm), (in)
d_0	The standard critical depth of cut under pre-defined standard cutting condition (mm), (in)
d_{max}	Maximum depth of cut in extra region of chip-breaking chart (mm), (in)
d_{min}	Minimum depth of cut in extra region of chip-breaking chart (mm), (in)
f	Feed rate (mm/rev), (in/rev)
f_0	The standard critical feed rate under pre-defined standard cutting condition (mm/rev), (in/rev)
f_{cr}	The critical feed rate (mm/rev), (in/rev)
f_{cr}	The critical feed rate (mm/rev), (in/rev)
h	Insert backwall height (mm), (in)
h_{ch}	Chip thickness (mm), (in)
K_{dbr1}	Modification coefficient of the cutting tool (insert) land length effect on the critical depth of cut
K_{dkr}	Modification coefficient of the insert lead angle effect on the critical depth of cut
K_{dm}	Modification coefficient of the workpiece material effect on the critical depth of cut
$K_{dr\varepsilon}$	Modification coefficient of the cutting tool (insert) nose radius effect on the critical depth of cut
K_{dT}	Modification coefficient of the cutting tool (insert) effect on the critical depth of cut
K_{dV}	Modification coefficient of the cutting speed effect on the critical depth of cut
K_{dWn}	Modification coefficient of the cutting tool (insert) chip-breaking groove width effect on the critical depth of cut
$K_{d\gamma 0}$	Modification coefficient of the cutting tool (insert) rake angle effect on the

critical depth of cut

$K_{d\gamma 01}$ Modification coefficient of the cutting tool (insert) land rake angle effect on the critical depth of cut

K_{fbr1} Modification coefficient of the cutting tool (insert) land length effect on the critical feed rate

K_{fh} Modification coefficient of the cutting tool (insert) backwall height effect on the critical feed rate

K_{fh} Modification coefficient of the cutting tool (insert) backwall height effect on the critical depth of cut

K_{fkr} Modification coefficient of the insert lead angle effect on the critical feed rate

K_{fm} Modification coefficient of the workpiece material effect on the critical feed rate

$K_{fr\varepsilon}$ Modification coefficient of the cutting tool (insert) nose radius effect on the critical feed rate

K_{fT} Modification coefficient of the cutting tool (insert) effect on the critical feed rate

K_{fV} Modification coefficient of the cutting speed effect on the critical feed rate

K_{fWn} Modification coefficient of the cutting tool (insert) chip-breaking groove width effect on the critical feed rate

$K_{f\gamma 0}$ Modification coefficient of the cutting tool (insert) rake angle effect on the critical feed rate

$K_{f\gamma 01}$ Modification coefficient of the cutting tool (insert) land rake angle effect on the critical feed rate

K_R Coefficient related to the chip radius breaking

l_b Backwall length (mm), (in)

l_f Chip / insert contact length (mm), (in)

l_n Rake face length (mm), (in)

R_0 Chip up-curl radius (mm), (in)

R_L Chip-breaking radius (mm), (in)

r_p Protruded nose radius (mm), (in)

R_s Side curl chip radius (mm), (in)

r_ε Insert nose radius (mm), (in)

V Cutting speed (sfpm)

w	The distance of center of protruded nose circle from insert nose radius center along insert symmetrical line (mm), (in)
W_n	Insert groove width (mm), (in)
W_{ne}	Inset equivalent groove width (mm), (in)
α	Insert nose angle (deg)
α_{ch}	Chip cross-section shape coefficient
γ_b	Insert backwall angle (deg) (deg)
γ_{be}	Insert equivalent backwall angle (deg)
γ_n	Insert rake angle (deg)
γ_{ne}	Insert equivalent rake angle (deg)
δ	Chip scroll angle in side-curl (deg)
ε	Workpiece fracture strain (mm), (in)
ε_B	Chip strain (mm), (in)
κ_r	Insert lead angle (deg)
η	Chip back flow angle (deg)
λ_s	Insert inclination angle (deg)
ψ_λ	Chip side flow angle (deg)

Table of Contents

List of Figures

List of Tables

1 Introduction

Machining chip-control has been overlooked in manufacturing process control for a long time. However, with the automation of manufacturing processes, chip-control becomes an essential issue in machining operations in order to carry out the manufacturing processes efficiently and smoothly, especially in today's unmanned machining systems and finishing operations.

On the three main areas of chip control study include chip formation, which covers chip flow and chip curl, and chip-breaking many experiments have been conducted. However given the complicated nature of chip formation, breaking and the progressive insert groove production, the results obtained from analysis do not match with industrial expectations. This chapter gives an overview in two categories; chip formation and chip breaking.

1.1 Overview of Chip Formation

After material is removed from the workpiece, it flows out in the form of chips. After flowing out, the chip curls either naturally or through contact with obstacles.

The most logical approach in developing cutting models for machining with chip-breaking is first to investigate and understand the direction of chip flow, since chip curling and the subsequent chip-breaking processes depend very heavily on the nature of chip flow and its direction.

For chip flow study, the most important objective is to establish the model of the chip side-flow angle, which in most research is called the chip flow angle. Figure 1-1 shows chip side flow angle.

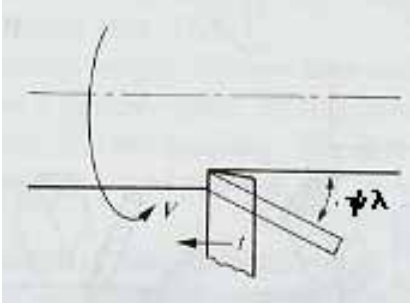

Figure 1-1 Chip Side Flow Angle (Stabler 1964)

Naturally a chip will curl after it flows out. Contact with the chip-breaking groove or chip breaker or other obstacles will also make a chip curl. There are three basic forms of chip curl, and combinations of these construct all chip shapes:

- Chip up-curl
- Chip side-curl
- Chip lateral-curl that was found in recent studies

The chip curl study requires the modeling of the chip up-curl and side-curl radii, both of which have very significant influences on chip-breaking. Figure 1-2 shows chip up-curl and side-curl.

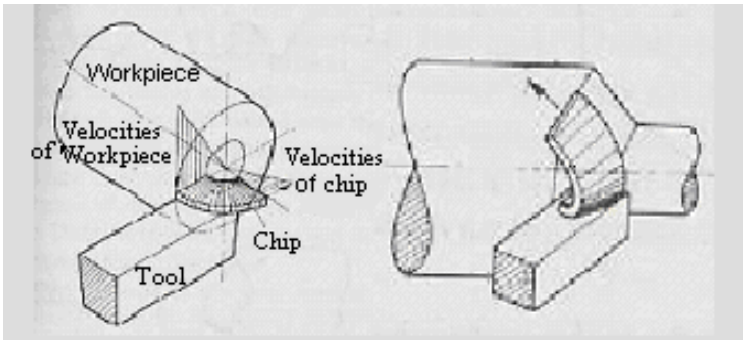

a) Chip Side-Curl **b) Chip Up-Curl**

Figure 1-2 Chip Side-Curl and Chip Up-Curl (Spaans 1971)

1.2 Overview of Chip Breaking

In machining chips that vary in shape and length, short broken chips are desired because:

- Operator's safety (in manual operation)
- Safety of machine tools and cutting tools
- Maintaining good surface finish on the machined surface
- Convenience of chip disposal
- Reduction of cutting temperature
- Increasing tool life and
- Possible power reduction

Therefore the study of chip-breaking is very important for optimizing the machining process. This importance is more significant in ductile materials such as soft gummy low carbon, tough steels leaded or resulfurized steels, and other soft materials and light cuts with positive rake angle tools.

Efficient chip-control will contribute to higher reliability of the machining process, a better-finished surface, and increased productivity.

Chip-breaking for brittle and ductile materials happen in different ways. When brittle metal such as cast iron and hard bronze are cut discontinuously segmented chips are produced naturally. As the point of the cutting tool contacts the metal, some compression occurs, and the chip begins flowing along the chip-tool interface. As more stress is applied to the brittle metal by cutting action, the metal compresses until it reaches a point where rupture occurs and the chip separates from the unmachined portion. This cycle is repeated indefinitely during the cutting operation, with the rupture of each

segment occurring on the shear angle or plane. Generally, as a result of these successive ruptures, a poor surface is produced on the workpiece.

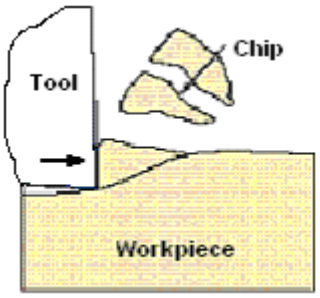

Figure 1-3 Chip Breaking in Brittle Materials

In each cycle of ductile materials chip breaking, a chip first flows out with some initial curling. Then the chip will keep on flowing out until it comes into contact with (simultaneously blocked by) obstacles like the work-piece surface or the cutting tool. The chip curl radius will then become larger and larger with the chip continuously flowing out. When the chip curl is tight enough to make the chip deformation exceed the chip material breaking strain, the old chip will break, and new chips will form, grow and flow out (see Figure 1-4).

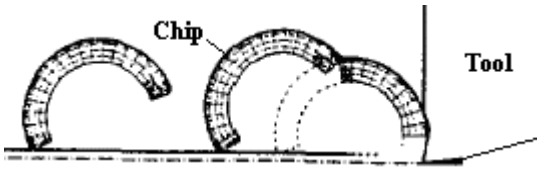

Figure 1-4 Chip-Breaking of Ductile Materials (Shinojukza, 2001)

Therefore the chip will break when the actual chip fracture strain (ε) is smaller than the tensile strain of the chip (ε_B),

The chip-breaking research includes many components and activities including:

- Workpiece material
- Tool geometry (including chip breaker features)

- Process parameters (built-up edge, vibration, force, heat, tool wear)
- Cutting condition (feed rate, depth of cut, cutting speed)
- Coolant

Figure 1-5 shows the main scope of chip-breaking study. Its goals are to: establish a chip-breaking model for prediction, design machining process, select tool, and design tool.

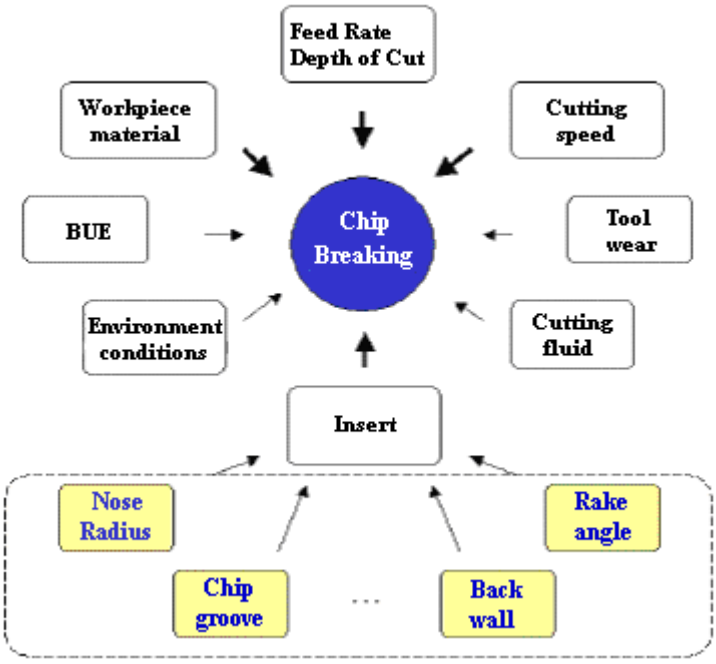

Figure 1-5 Research Fields of Chip-Control (Zhou 2001)

To break chips by mechanical obstacles there are two main chip-breaking modes: chip-breaking by chip/work-surface contact and chip-breaking by chip/tool flank-surface contact (Figure 1-6). In the first mode a chip may break by contact with the surface to be machined, which is caused by chip side-curl (Figure 1-6e). It can also, break by contact with the machined surface (shoulder of workpiece) caused by chip up-curl (Figure 1-6a,

1-6b). The second breaking mode chip breaks by contact with the flank-surface caused by both chip up (Figure 1-6c) and side curl (Figure 1-6d)

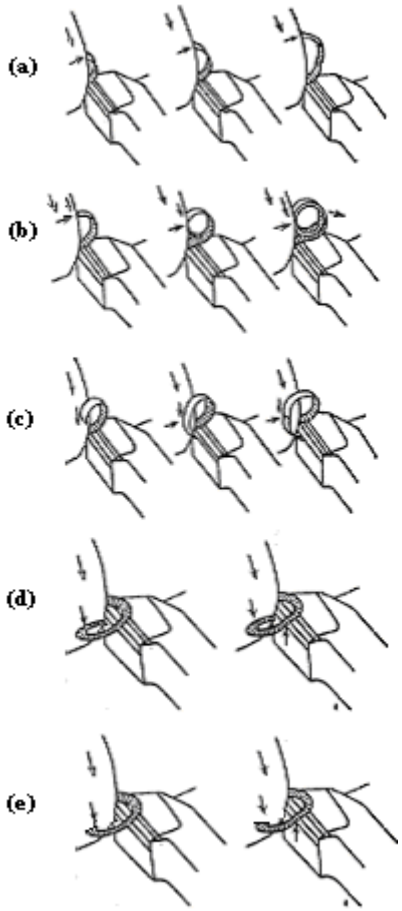

Figure 1-6 Modes of Chip Breaking (Nakayama 1960)

In this thesis the chip-breaking in up-curl chips is studied, and later on this type of chip formation and breaking will be analyzed in detail.

There are three major factors that affect chip breaking:

- Change cutting conditions (feed rate, depth of cut, cutting speed)
- Change cutting tool geometric features (nose radius, rake angle, lead angle)

- Design and use a chip breaker or chip-breaking groove (groove width, backwall height, backwall angle)

Increasing the depth of cut or the feed rate can significantly improve chip breakability. However, in industry this is not practical in finish cutting due to the limitations of the machining process. Therefore, optimizing the design of the cutting tool's geometric features and the chip breaker / chip-breaking groove is the most plausible and efficient way to break the chip.

2 Literature Review of Chip Formation and Breaking

This chapter reviews both previous work done by researchers on fundamentals of chip-formation and breaking, and attempts to develop chip-breaking criteria. The Nakayama's chip-breaking criterion, and Li's work on chip-breaking limits are reviewed in detail. This is particularly important because the chip-breaking predictive models developed in this thesis are based on chip-breaking limits theory and on Nakayama's work. Finally, existing problems in chip-control and formation models are also reviewed.

2.1 Chip Flow

Chip-breaking modes depend on the nature of chip flow and its direction. Understanding the chip flow mechanism is important for chip-control. Chip flow is determined by many factors and is usually described by the chip flow angle (ψ_λ). The chip-flow angle is the angle between the chip-flow direction on the cutting tool rake-face and the normal line of the cutting edge (see Figure 2-1). Establishing the model of the chip flow angle is the main objective of chip flow research. Due to the extreme complexity of the chip formation process, only limited success has been achieved in chip-flow research, especially in three-dimensional conditions (three-dimensional groove, and three-dimensional cutting).

A lot of work has been done on chip-flow angle research during the last few decades, and there are many methods for calculating the chip-flow angle. The investigation of chip flow began with modeling over plane rake face tools.

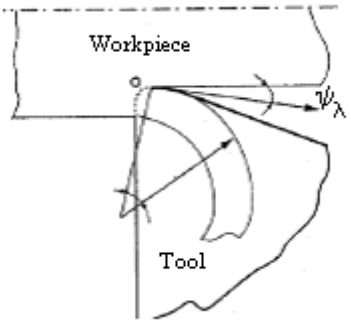

Figure 2-1 Chip Side Flow Angle (Jawahir, 1993)

Merchant, Shaffer and Lee used the plasticity theory to attempt to obtain a unique relationship between the chip shear plane angle, the tool rake angle and the friction angle between the chip and the tool (Merchant, 1945; Lee, 1951). Shaw (1953) proposed a modification to the model presented by Lee and Shaffer. Palmer (1959) presented the shear zone theory by allowing for variation in the flow stress for a work-hardening material. Van Turkovich (1967) investigated the significance of work material properties and the cyclic nature of the chip-formation process in metal cutting. Slip line field theory is widely applied in chip-formation research and some slip-line field models are presented (Usui, 1963; Johnson, 1970; Fang, N. 2001). Being computationally successful, slip line field models do not agree well with experiment results due to lack of knowledge of the high strain rate and temperature flow properties of the chip material.

Through studying the chip flow in free oblique cutting, Stabler presented a famous rule called the "Stabler Rule" (Stabler, 1951):

$$\psi_\lambda = K\kappa_r \qquad (2\text{-}1)$$

where the ψ_λ is the chip side flow angle, the κ_r is the cutting-tool inclination angle, and K is a material constant. This rule is applicable for free oblique cutting.

Another chip flow model is presented with the assumption that the chip flow is perpendicular to the major axis of the projected area of cut. This model uses empirical substitutions to consider the effect of cutting forces (Colwell, 1954). i.e.

$$\psi_\lambda = \tan^{-1}\left(\frac{\sqrt{2r_\varepsilon d - d^2} + f/2}{d}\right) \qquad \frac{d}{r_\varepsilon} < (1-\cos\kappa_r) \tag{2-2}$$

$$\psi_\lambda = \tan^{-1}\left(\frac{d/\tan\kappa_r + r_\varepsilon \tan(\kappa_r/2) + f/2}{d}\right) \qquad \frac{d}{r_\varepsilon} \geq (1-\cos\kappa_r) \tag{2-3}$$

where d is depth of cut, κ_r is insert lead angle, f is feed rate, and r_ε is nose radius (see Figure 2-2).

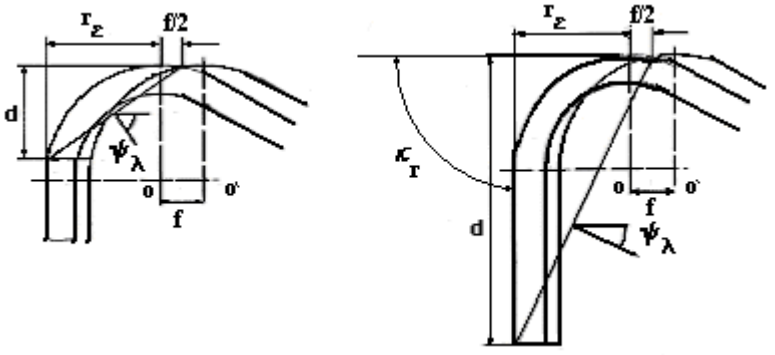

Figure 2-2 Chip Side Flow Angle According to Colwell Theory

Later on the groove parameters will be defined along the side flow angle. Since Colwell's equation does not consider the effect of the work-piece material, this model therefore will result in significant error under particular conditions.

Okushima considered that chip flow is invariant with cutting speed and chip flow should be the summation of elemental flow angles over the entire length of the cutting edge (Okushima, 1959).

A chip flow model was presented by Young in 1987, assuming Stabler's flow rule, with validity for infinitesimal chip width, and the directions of elemental friction forces summed up to obtain the direction of chip flow (Young 1987).

The above chip flow studies are shown in Figure 2-3.

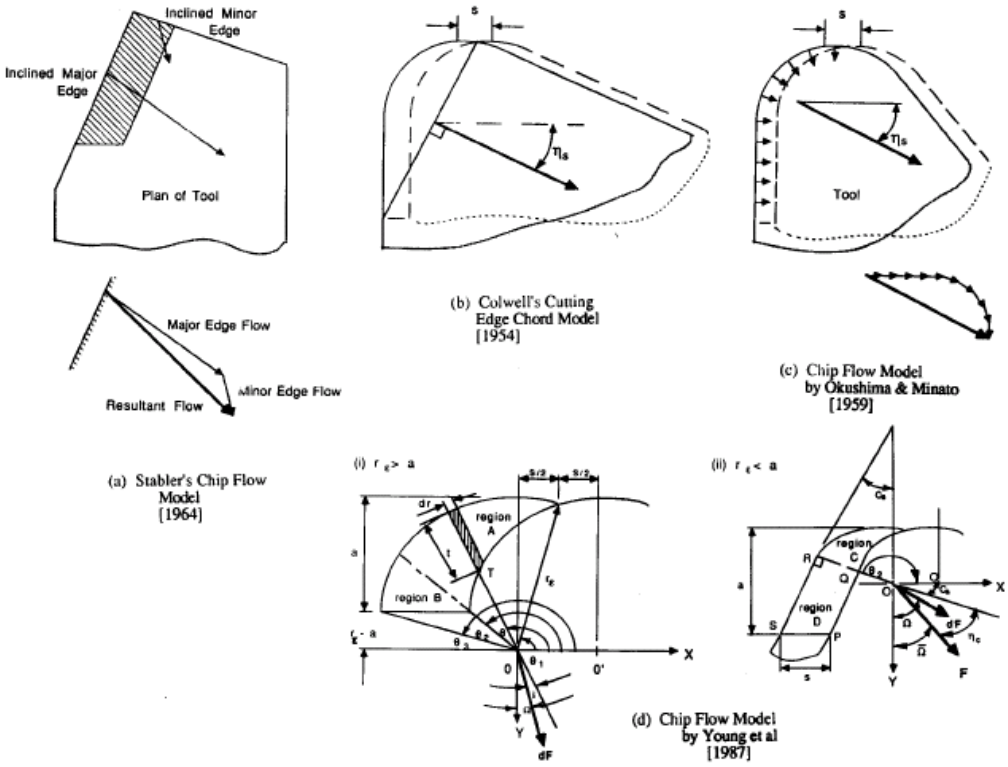

Figure 2-3 Chip Flow Models for Machining with a Flat-Faced Tool (Jawahir 1998)

Jawahir et al (1988-a) found that a chip also has another form of flow angle, which he called chip back flow angle (η) show in Figure 2-4. However in real machining condition the chip flows in 3-D space with both side and back flow angles.

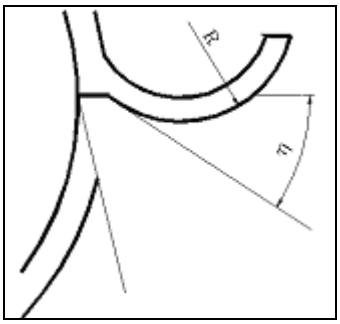

Figure 2-4 Chip Back Flow Angle

2.2 Chip Curl

Chip flow is only a part of chip space movement. To understand the chip movement mechanism, it is necessary to study chip curl. Chip curl has two basic modes: up-curl and side-curl. Recently the third chip curl mode called lateral curl was found (Fang, 2001). The chip up-curl is much simpler than the other two kinds of chip curl. Therefore, the greatest achievements have been in chip up-curl modeling. Chip side-curl is much more difficult than up-curl and currently there are no applicable models of the chip side-curl.

2.2.1 Chip Up-Curl

The up-curl chip is chip that curves in the plane which is defined by chip flow direction and perpendicular to the cutting edge. The up-curl curve is described with chip up-curl radius R_o. Nakayama considered that when there is a build-up edge on the cutting tool, the part of the chip that flows over the build-up edge would come in contact with the tool rake-face, which brings a bent moment to the chip (Nakayama, 1962-b). For the grooved tool, the chip-breaking groove can help chip curl (see Figure 2-5).

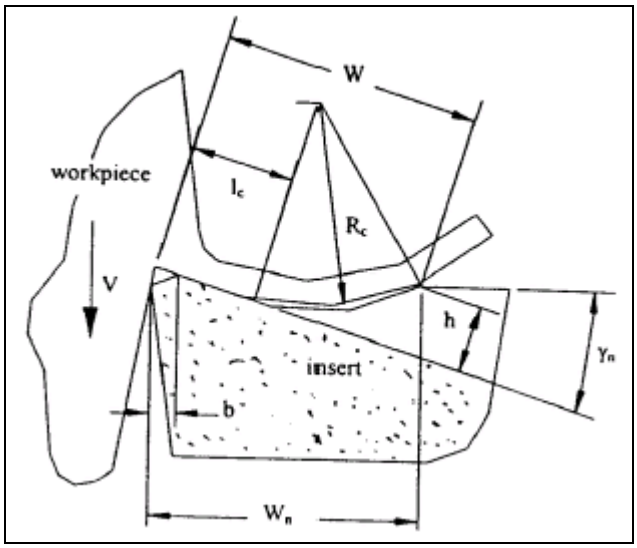

Figure 2-5 Chip Up-Curl Process with Grooved Cutting Tool (Li. Z 1990)

The following is the chip-up curl radius (R_0) equation given by Jawahir et al (1988-e)

$$R_0 = R \tag{2-4}$$

where *R* is the chip-breaking groove radius. In this equation it is assumed that the chip back flow angle η is very large or the restricted contact length is small so that the chip flows through the whole chip-breaking groove (Figure 2-6a). If the chip back flow angle (η) is small or the restricted contact length is long, the chip does not flow through the whole chip-breaking groove. In that case the up curl radius equation according to Jawahir et al is (1988-e):

$$R_0 = K_{ch} \frac{W_n}{2\sin\eta} \tag{2-5}$$

where K_{ch} is a constant determined by the chip material, W_n is groove width and η is chip back flow angle (Figure2-6b).

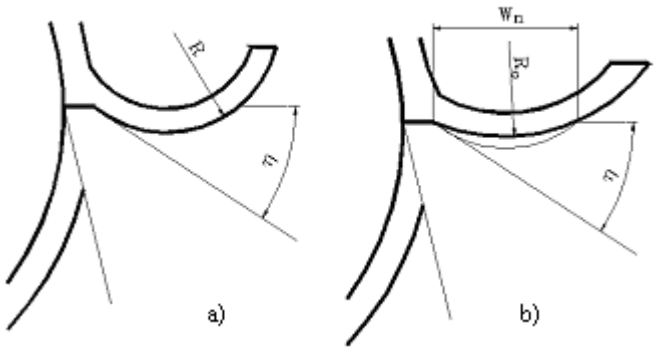

Figure 2-6 Chip Radii According to Jawahir (1988-e) Theory

Based on chip-cutting tool geometric analysis, Li et al (1990) presented a chip up-curl radius equation where the insert rake angle was considered as the chip flow entrance angle in the groove. Here the chip-tool contact length on the groove body is taken into account.

$$R_o \approx \frac{W_n}{2\sin\gamma_n}\left(1 - 2\frac{l_f}{W_n}\cos\gamma_n\right) \tag{2-6}$$

where l_f is the chip/tool contact length, and γ_n is the rake angle. It is noticeable that this equation is not affected by groove profiles, which are not necessarily a portion of the circle. Also this equation is for insert grooves in which the backwall height is zero.

Zhou (2001-a) added the insert groove backwall height as shown in Figure 2-7 and formulated this equation:

$$R_o \approx \frac{{W_n}^2 + h^2 + {l_f}^2 + 2l_f\left(-W_n\cos\gamma_n + h\sin\gamma_n\right)}{2(W_n\cos\gamma_n + h\sin\gamma_n)} \tag{2-7}$$

where h is backwall height.

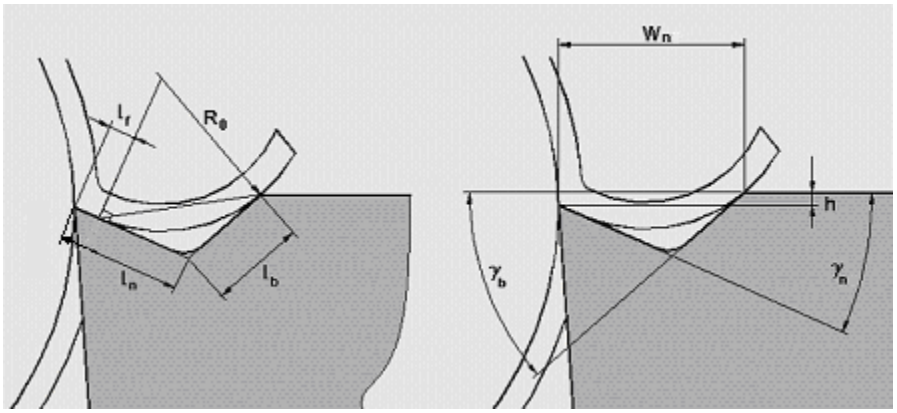

Figure 2-7 Chip Up-curl Formation According to Zhou et al Theory (Zhou 2001-b)

2.2.2 Chip Side-Curl

Chip side-curl (R_s) is the chip curl in the direction of chip width. The side-curl axis is generally perpendicular to the chip bottom surface. The chip side-curl is caused by differences in the material flow speed along the chip width direction on the chips bottom surface (see Figure 2-8).

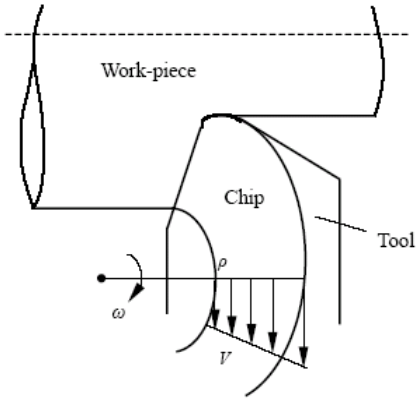

Figure 2-8 Mechanism of Chip Side-Curl (Zhou 2001-b)

The chip side-curl radius has a critical influence on side-curl-dominated chip-breaking. The main objective of chip side-curl research is to establish the model of the chip side-curl radius.

Nakayama considered that the chip material had side flow, which leads to chip side-curl. He also considered that the thicker the chip, the greater the chip material side flow, therefore the greater the chip side-curl. He proposed the following side-curl radius equation,

$$\frac{1}{R_S} = \left(\frac{0.75}{b_{ch}} - \frac{0.09}{h_{ch}} \right) \frac{1}{k} \tag{2-8}$$

where b_{ch} is the chip width and h_{ch} is the chip thickness. (Nakayama 1990)

2.2.3 Chip Lateral-Curl and Combination Chip Curl

Chip lateral-curl was identified by Fang N. (2001). It may appear in a very special condition. There is no model built up for chip lateral-curl yet. In real cases, the chip curl form is a combination of the two basic curl forms: up-curl and side-curl.

2.3 Chip-Breaking Criterion

As discussed in Chapter 1, chip-breaking has two basic modes: chip-breaking by chip/work surface contact or chip-breaking by chip/tool flank surface contact. For chip-breaking research, we need to set up the chip-breaking criteria; for industry application, we need to find efficient ways to break chips.

The following is a summary of the two approaches of chip-breaking research:

1. Material stress analysis – to find the chip-breaking strain ε_B.

Research work by this approach includes:

• Chip curl analysis (Nakayama, 1962; Li, 1990)

• Finite Element Analysis or FEA (Kiamecki, 1973; Lajczok, 1980; Strenkowski, 1985; etc.)

2. Experiment-based work

This approach uses the database system established by Fang and Jawahir which is based on fuzzy mathematical model for chip breakability assessments (Fang, 1990-a, Jawahir, 1989).

This approach requires lots of time, money, and labor to establish the chip breaking prediction database. With new work-piece materials, new cutting tools / lathe, and new machining methods constantly coming out, it is difficult to establish and maintain a chip-breaking database for prediction.

Tool designers optimize their tool design based on many cutting tests. In the industry machining process, some special devices such as a rotating knife, a high-pressure gas/fluid jet and a vibrating cutting tool are also designed to break the chip. However, the most efficient and most common way to break the chip is to use the chip-breaking groove /chip breaker and optimize geometric features of the cutting tool.

Presently, there has been only limited success in the chip-breaking criterion study. The theoretical achievements fall behind industry reality and requirements.

Nakayama (1962-b) presented the most common chip-breaking criteria for up-curl-dominated chips. Presently most research on chip-breaking criteria are for two-dimensional chip-breaking. The chip-breaking criteria for three-dimensional chip-breaking needs further investigation. Three-dimensional chip-breaking criteria can not be established without a reasonable two-dimensional chip-breaking model.

The finite element method has been applied in the chip-breaking process analysis for plane rake-face and grooved tools for orthogonal machining, and most recently for three-dimensional machining (Kiamecki, 1973; Lajczok, 1980; Strenkowski, 1985,

1990). These analyses are computationally successful, but their predictions do not agree with the experiments.

Nakayama's chip-breaking criterion is the most common. Therefore it is reviewed in detail.

Nakayama considers that when the actual chip fracture strain (ε) is smaller than the tensile strain of the chip (ε_B), the chip will break. It is noted that the ε is proportional to the ratio of chip thickness and chip curl radius. i.e. (Li. Z 1990) :

$$\varepsilon_B \propto \frac{h_{ch}}{R_0} \tag{2-8}$$

where h_{ch} is the chip thickness, R_0 is the chip up-curl radius.

Nakayama considered that a chip flows out with up-curl radius R_0, and then is blocked by the work-piece surface or the cutting tool. With the chip material continuously flowing out, the chip curl radius will be increasing continuously. When the chip reaches up-curl radius R_L where the chip actual fracture strain ε is smaller than the chip strain ε_B, the chip will break

When the chip cross-section shape is a rectangle, ε_B can be calculated by the following equation (Li, 1990):

$$\varepsilon_B = \frac{h_{ch}}{2}\left(\frac{1}{R_0} - \frac{1}{R_L}\right) \tag{2-9}$$

Otherwise, the above equation can be written as Nakayama (1962-b):

$$\varepsilon_B = \alpha_{ch} h_{ch}\left(\frac{1}{R_0} - \frac{1}{R_L}\right) \tag{2-10}$$

where α_{ch} is cross-section shape coefficient; and h_{ch} is the chip thickness.

2.4 Li's Work on Chip-Breaking

Developing a reasonable chip-breaking criterion is the prerequisite for establishing an applicable chip-breaking predictive model. However the extreme complexity of the chip-breaking process makes the theoretical analysis and modeling of chip-breaking very difficult. Based on Nakayama's work and chip-breaking limits theory, through chip curl analysis, Li (1990) presented a new semi-empirical chip-breaking prediction model.

Since it is the basis of the chip-breaking prediction models developed in this research, it will be reviewed in detail in the following section. To better understand the model, first the chip-breaking chart is introduced.

2.4.1 Chip Breaking Chart

Below are the chip breaking curves and chip type classifications based on observations from previous study involving a large number of experiments (Figure 2-9).

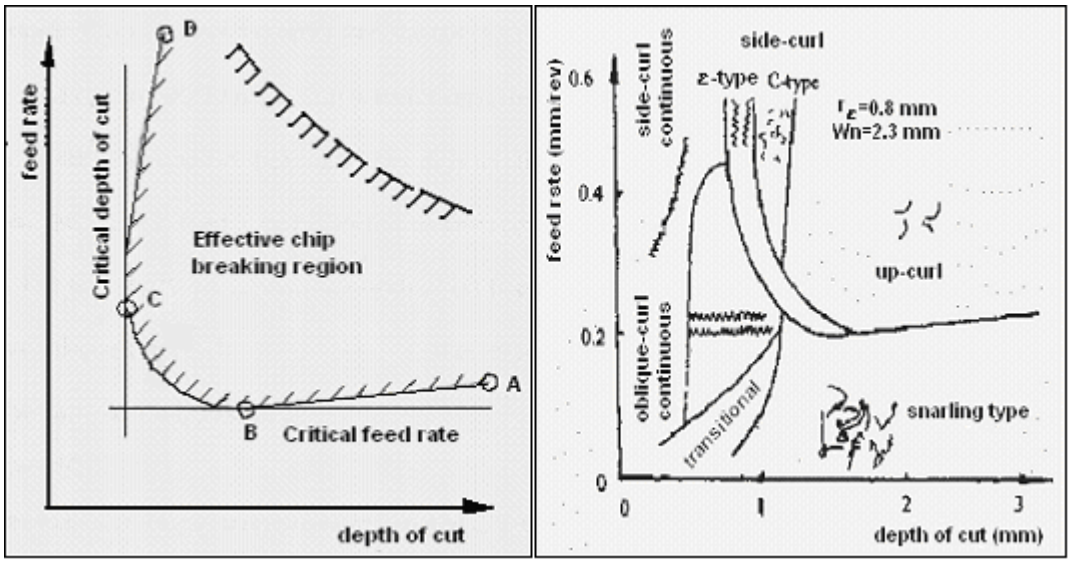

a) **b)**

Figure 2-9 Typical Chip Breaking Charts (Li, 1990)

The graph shows that there are critical feed rates and critical depth of cuts. When the depth of cut is greater than the critical depth of cut and the feed rate is greater than critical feed rate, the chip will break. Otherwise a long chip will be produced. For specific workpiece materials, cutting tools and cutting speed, the chip-breaking chart is consistent. Generally the chip-breaking curve can be divided into three typical parts (see Figure 2-9a) up-curl dominated chip-breaking region AB, side-curl dominated chip-breaking region CD, and transitional region BC. Because of a complicated nature of chip in BC, the curve in CD and AB only is analyzed and the relevant equations are detailed in this chapter.

Side Curl Dominant Region CD

The region CD of the chip-breaking curve shown in Figure 2-9a includes side-curl dominated chip formation and breaking processes. Side curl chip is the chip curl in the direction of the chip width. The side curl axis is generally perpendicular to the chip's bottom surface (see Figure 2-7). This region shows a complex 3-D chip curling. On each side of the limit, the broken area is mainly of side-curled spiral type continuous chips.

Up-Curl Dominant Region AB

In the region AB of the chip-breaking curve shown in Figure 2-9a, the lowest point, B, is the minimum or critical feed rate. This region is primarily a straight line with a slope and with regard to Figure 2-9, can be analyzed as a 3-D chip-up-curling dominant process. So the definition of up-curl chip is the chip curl in the chip thickness direction, the axis of chip curl approximately parallels the chip/cutting tool rake face detachment line.

Based on Nakayama's work and chip-breaking limits theory, through chip curl analysis, Li (1990) presented a new theoretical and semi-empirical chip-breaking model.

Since it is the basis of the chip-breaking models developed in this research, they are reviewed in detail in the following parts.

- Theoretical Analysis method
- Semi-Empirical predictive method

2.4.2 Theoretical Analysis of Critical Feed Rate and Depth of Cut

As it was explained in chip-breaking chart: *The chip will always break when the depth of cut is greater than the critical depth of cut (d_{cr}), and the feed rate is greater than the critical feed rate* (f_{cr}). *Otherwise, the chip will not break.*

In Nakayama's model (Equation (2-10)), for up-curl dominated chip-breaking region, the chip thickness (h_{ch}) can be calculated as:

$$h_{ch} = \frac{f \sin \kappa_r}{C_h} \tag{2-12}$$

where κ_r is the insert lead angle, C_h is the cutting ratio.

Substituting h_{ch} into Equation (2-10), the following equation is established for **critical feed rate** (f_{cr}):

$$f_{cr} = \frac{\varepsilon_b}{\alpha_{ch}} \cdot \frac{C_h K_R R_0}{\sin \kappa_r} \tag{2-13}$$

where K_R is the coefficient related to the chip radius breaking:

$$K_R = R_L / (R_L - R_0) \tag{2-14}$$

When $f > f_{cr}$, the chip will break. Similar to f_{cr}, a **critical depth of cut** (d_{cr}) can be defined for the side-curl-dominated chip-breaking region (see Figure 2-10). The equation of d_{cr} for two-dimensional grooved inserts is as follows (Li, 1990):

$$d_{cr} = \frac{\varepsilon_B R_s \cos\delta}{\alpha} - \left(\frac{\pi}{2} - 1\right) r_\varepsilon \quad \text{for} \quad d \geq r_\varepsilon \tag{2-15}$$

$$d_{cr} = \left(\cos\frac{57.3\varepsilon_B R_s \cos\delta}{\alpha r_\varepsilon}\right) - r_\varepsilon \quad \text{for} \quad d < r_\varepsilon \tag{2-16}$$

where R_s is the radius of side curl chip (Equation (2-8)); α and δ are a chip's cross sectional related parameters and r_ε is the insert nose radius.

In critical depth of cut equations insert nose radius is the major parameter that affects critical depth of cut.

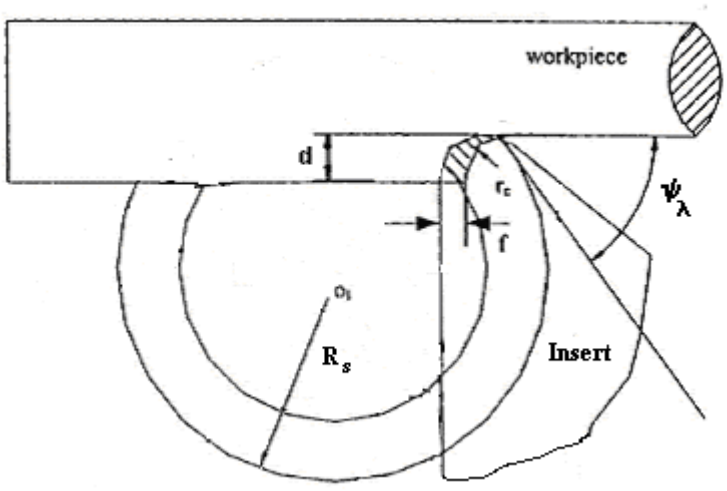

Figure 2-10 Chip Flow of Side-Curl Dominated ε-Type Chips (Zhou 2001-b)

Although in practical, the critical depth of cut is affected by groove parameters (Zhou 2001-b) but the groove parameters have no role in chip side curl formation and

chip radius dimension. In this study more concentration will be given on up-curl dominant chip formation, which explicitly affected by insert specifications.

Equation (2-13) does not satisfy real machining conditions, which chip formation occurs in 3-D with 3-D groove. Therefore in this thesis critical feed rate equation (Equation (2-13)) will be improved to 3-D with 3-D groove. As well in conditions that the depth of cut is smaller than the nose radius (e.g. $d<r_\varepsilon$), critical feed rate (f_{cr}) will be modified.

2.4.3 Semi-Empirical Chip-Breaking Predictive Model

The theoretical equations of d_{cr} and f_{cr}, shown above, cannot be used directly to predict chip-breaking limits because not all parameters in the equation can be calculated directly. Therefore a semi-empirical chip-breaking predictive model based on theoretical equations of d_{cr} and f_{cr} was presented (Li, 1990) for industry application.

The chip-breaking limits are influenced by a lot of factors but are mainly determined by the work-piece material, cutting speed, and insert geometric features (see Figure 2-11).

Applying the single-factor modeling method, Li presented the following chip-breaking predictive model:

$$\begin{cases} f_{cr} = f_0 K_{ft} K_{fV} K_{fm} \\ d_{cr} = d_0 K_{dt} K_{dV} K_{dm} \end{cases} \tag{2-17}$$

where f_0 and d_0 is the standard critical feed rate and the standard critical depth of cut under a predefined standard cutting condition.

The predefined standard cutting condition can be defined with a certain workpiec material, groove parameters and surface speed. K_{fT} and K_{dT} are the cutting tool (inserts)

effect coefficients; K_{fV} and K_{dV} are the cutting speed effect coefficients; and K_{fm} and K_{dm} are the work-piece material effect coefficients. The empirical coefficients K_{dm}, K_{dV}, K_{dT}, K_{fm}, K_{fV}, and K_{fT} are developed through cutting tests. Once the empirical equations of K_{dm}, K_{dV}, K_{dT}, K_{fm}, K_{fV}, and K_{fT} have been set up, they can be calculated when the cutting condition is specified. Then the f_{cr} and d_{cr} can be figured out under any conditions by multiplying the f_0 and d_0 with K_{dm}, K_{dV}, K_{dT}, K_{fm}, K_{fV}, and K_{fT}, respectively. Therefore the chip-breaking can be predicted under any given cutting condition.

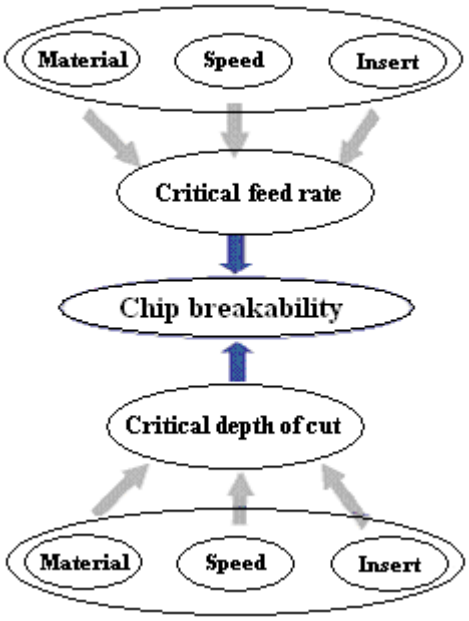

Figure 2-11 Factors Influence Chip Breaking (Zhou 2001-b)

Work-Piece Material Coefficients K_{dm} and K_{fm}

For estimating the work-piece material constant Equations (2-18) can be used.

$$\begin{cases} K_{fm} = f_{cr} / f_0 \\ K_{dm} = d_{cr} / d_0 \end{cases} \tag{2-18}$$

First, conduct a group of cutting tests under predefined conditions with the given work-piece material to obtain a group of d_{cr} and f_{cr}. Dividing them by the d_0 and f_0, the

K_{dm} and K_{fm} can be estimated. Collecting all K_{dm} and K_{fm} for different work-piece materials, a work-piece material coefficients database can be set up.

Cutting Speed Coefficients K_{dV} and K_{fV}

For set up the cutting speed empirical equations, Equations (2-19) can be used.

$$\begin{cases} K_{fV} = f_{cr} / f_0 = a_f V + b_f \\ K_{dV} = d_{cr} / d_0 = a_d V + b_d \end{cases} \tag{2-19}$$

First, conduct several groups of cutting tests under predefined conditions, except changing the cutting speed for several levels. Then we can get several groups of d_{cr} and f_{cr}; dividing them by the d_0 and f_0, we can then get several K_{dV} and K_{fV}. Then we can use curve-fit to develop the general empirical equations for the K_{dV} and K_{fV}. After the empirical equations are established we can estimate K_{dV} and K_{fV} for any cutting speed without conducting any extra cutting tests.

If the predefined standard condition is different, the above equations of the K_{dV} and K_{fV} should multiply by a constant respectively.

Insert Geometric Coefficients K_{dT} and K_{fT}

Li (1990) set up the K_{dT} and K_{fT} models for two-dimensional grooved inserts as follows. The predefined standard condition is still the same as before. The K_{dT} and K_{fT} are developed as functions of the insert nose radius r_ε, the chip-breaking groove width W_n and the insert lead angle k_r.

$$K_{fT} = K_{fr\varepsilon} K_{fkr} K_{fWn} \tag{2-20}$$

where $K_{fr\varepsilon}$ is the nose radius effect coefficient, K_{fkr} is the rake angle effect coefficient, and K_{fWn} is the width of the chip-breaking groove effect coefficient.

$$K_{dT} = K_{dr\varepsilon} K_{dkr} K_{dWn} \tag{2-21}$$

where $K_{dr\varepsilon}$ is the nose radius effect coefficient, K_{dkr} is the insert lead angle effect coefficient, and K_{dWn} is the width of the chip-breaking groove effect coefficient. In this research, an improved model based on Li's model will be developed, which will be described in Chapter 5.

2.4.4 Chip Breaking Chart for Inserts with Complicated Geometry

The definition of critical feed rate and depth of cut offered by Li et al, with regard to Figure 2-12 (Zhou 2001-b), does not cover all types of inserts. There is area that although related depth of cut and feed rate is smaller than critical feed rate and depth of cut of normal region, the chip is broken.

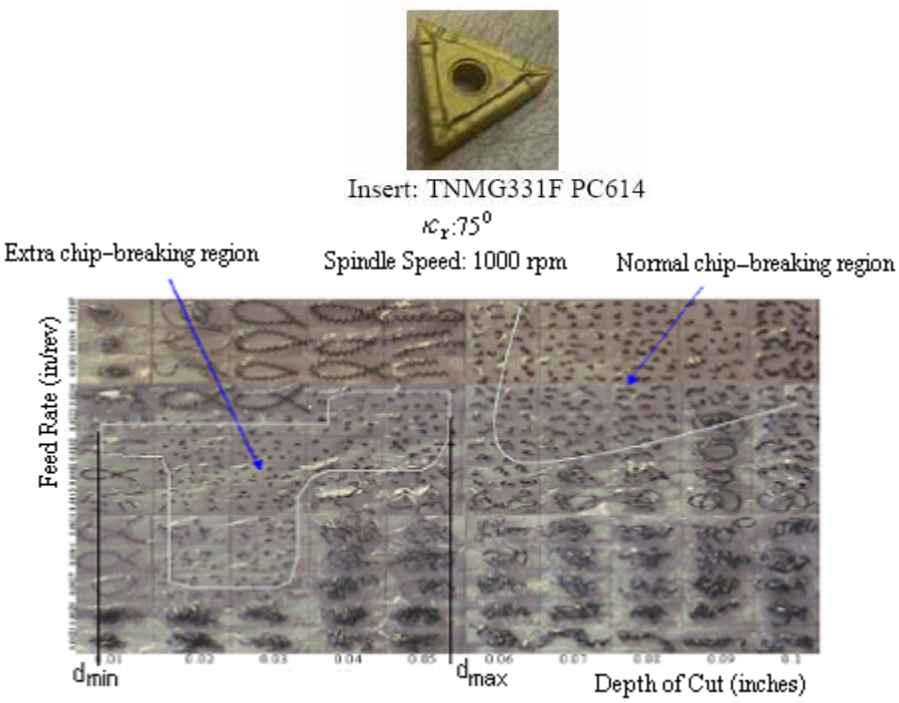

Figure 2-12 A Sample Chip Breaking Chart Produced by Complicated Groove Inserts (Zhou 2001-b)

In this thesis for extra chip-breaking region the depth of cut at the beginning of the region called minimum depth of cut and the depth of cut at the end of the region

called maximum depth of cut (Figure 2-12). Therefore a new method should be defined and established to explain the phenomena that differ the chip-breaking chart in Figure 2-12 from ordinary ones introduced in above section (see Figure 2-9). The next section will discuss the chip-breaking groove and the cutting tool classification.

2.5 Chip-Breaking Groove & Cutting Tool Classification

With regard to different application of inserts, related chip-breaking grooves vary greatly. To analyze the chip-breaking groove's effects on metal cutting, the chip-breaking groove needs to be classified first. In Zhou dissertation (2001-b), different cutting tools are classified based on different types of chip-breaking features. He classified the cutting tool into five categories: flat rake face tools, tools with block type chip breaker, tools with two-dimensional chip-breaking groove, tools with 3-D chip-breaking groove, and tools with complicated geometry modifications. Figure 2-13 illustrates the five kinds of cutting tools. (Zhou 2001-b).

In present research work inserts with 3-D groove type chip breakers are categorized in more detail. The inserts with three-dimensional grooves are divided into two types: simple and protruded insert groove; the simple grooves are grooves, which from top view show sides that are parallel with insert edges, as shown in Figure 2-14.

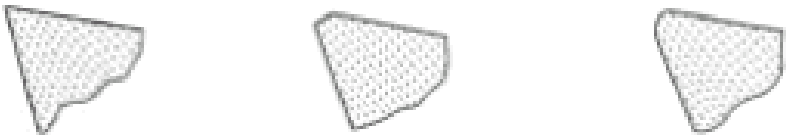

(i) Straight Cutting Edge (ii) Chamfered Cutting Edge (iii) Rounded Cutting Edge

(a) Flat Rake Face Tool (Jawahir, 1993)

(b) Insert with Block Type Chip Breaker

(c) Insert with Two-Dimensional Chip-Breaking Groove

(d) Inserts with Three-Dimensional Chip-Breaking Groove

(e) Inserts with Complicated Geometry Modifications

Figure 2-13 Classification of Chip Breaker / Chip-Breaking Groove (Zhou 2001-b)

In this type of grooves, the groove related parameters should be considered along a section perpendicular to the insert side edges. There are two set of parameters

associated with grooves namely V type groove section profile and a arc profile (see Figure 2-15).

(i) CNMG432-91 NL92 (ii) TNMG 332-23 4035

a) Inserts with Simple Groove

i) TNMP 332K KC850 ii) TNMG 332 QF 4025

b) Inserts with Protruded Groove

Figure 2-14 Inserts with Three-Dimensional Chip-Breaking Groove

The parameters of the V type section include: groove width (W_n), rake angle (γ_n), backwall angle (γ_b) and backwall height (see Figure 2-15a) and similarly for a portion of circle section profile are groove width (W_n), insert/chip restricted contact length ($b_{\gamma 1}$), rake angle (γ_n) and groove radius (see Figure 2-15b).

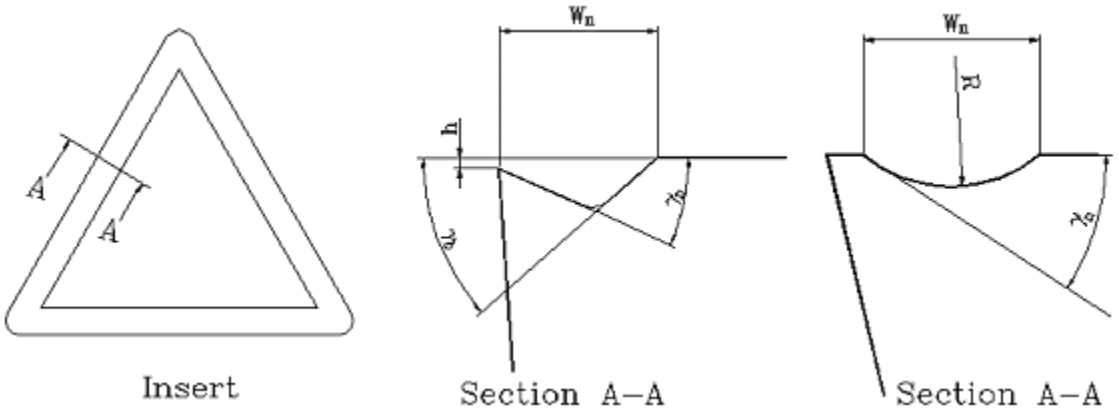

a) **b)**

Figure 2-15 Simple Groove Nominal Parameters and Profiles

In Protruded type groove inserts, there are two subcategories: sharp protruded nose (Figure 2-14bi) and round protruded nose (Figure 2-14bii).

For both of them the groove parameters should be considered along the symmetric line of the insert as shown in Figure 2-16.The parameters include: groove width (W_n), rake angle (γ_n), backwall angle (γ_b), backwall height (h) and insert/chip restricted contact length $b_{\gamma 1}$.

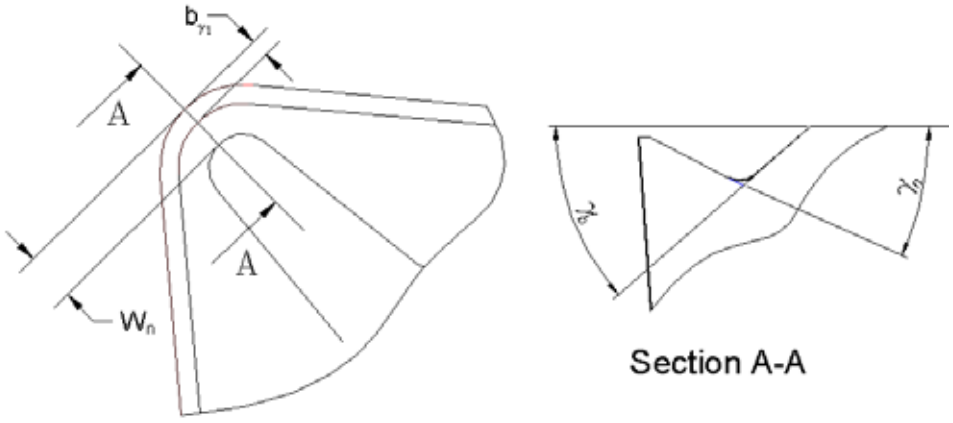

Figure 2-16 Protruded Groove Nominal Parameters

In this thesis, both the chip formation in different type groove profile section is and the chip breaking chart in protruded type grooves are analyzed.

2.6 Existing Problems

For today's unmanned manufacturing systems, chip-control needs to be considered as important as tool wear, cutting forces, surface finish, and machining accuracy. It is essential to develop an efficient chip-breaking prediction tool to optimize the machining processes. Presently, a big gap still exists between analytical work and practical requirements in the chip-control field. Two main problems exist in the chip-breaking prediction research:

1. In the chip-breaking, theoretical equation of f_{cr} is for 2-D up-curl and does not cover 3-D chip curl with side flow angle.

Li and Zhou's work on f_{cr} theoretical equation model is for 2-D and the backwall angle and efficiency of groove width which can have significant influence on chip-breaking, are not included in the model.

2. Lack of precise chip-breaking prediction model for inserts with 3-D groove.

3-D groove, especially the protruded type, inserts are the most popular inserts in finish cutting in industry. It is crucial for chip-control to establish an efficient and precise chip-breaking prediction model for three-dimensional grooved inserts.

3 Objectives and Scope of Work

3.1 Objectives

The objective of this research is to improve the chip-breaking predictive model for oblique turning with 3-D groove inserts. It contains two parts:

1. Extending Zhou's chip up-curl radius model for 2-D grooved inserts to include important geometric features of groove.

The effects of the cutting tool's backwall length to rake land length ratio and backwall angle, which are important for chip-breaking but are not considered in Zhou's model, are studied and included in the expanding model.

2. Developing and detailing a chip-breaking predictive model for critical feed rate in 3-D cutting with 3-D groove inserts.

The chip-breaking problems mainly exist in the finish cutting, where the depth of cut is small. More than 70% of the industry inserts used in finish cutting are three-dimensional grooved inserts. The particular significance of this work is that it presents a model for critical feed rate that covers real machining conditions in 3-D with 3-D groove.

3.2 Approach

Chip-control is very important to optimize the machining process. Developing an efficient chip-breaking predictive tool is essential to the machining industry. The tool should fulfill the following industrial requirements:

1. Predict whether a chip breaks under given cutting conditions when the cutting tool is specified.

2. Optimize cutting-tool and cutting condition designs to break a chip.

Presently, there is a big gap between the theoretical research and the stated above industrial requirements. Most industry cutting processes employ oblique cutting with three-dimensional grooved cutting tools, while most successful analytical models are for orthogonal cutting with simple grooved tools. For oblique cutting with three-dimensional grooved cutting tools, there is a lack of fully reasonable chip-breaking criterion. Presently database systems are used for chip-breaking prediction and a "try and see" method is used for tool design/selection in industry applications. However, methods are very costly.

The semi-empirical chip-breaking model approach (Li, 1990), shown in the Chapter 2, is a practical way to bridge the gap, with great advantages including:

1. It concentrates on the chip curl process instead of the chip formation process so it avoids the analyzing of the extremely complicated chip flow area.
2. Supported by the chip-breaking limits theory, it only needs to consider the up-curl dominated chip-breaking process and the side-curl dominated chip-breaking process for chip-breaking analyzing. Thus the problem is greatly simplified.
3. It does not fully rely on theoretical analysis. Instead, it uses limited cutting tests to develop the semi-empirical equations of chip-breaking limits. The number of cutting tests needed to develop the semi-empirical models is greatly reduced in comparison with present industry chip-breaking databases.
4. The semi-empirical chip-breaking model is intended for oblique cutting with grooved cutting tools, which is an appealing solution for industry application.

Given these advantages, the following steps are applied in this research.

1. The parameters that have influence on the chip formation are analyzed in detail on critical feed rate in 2-D groove first.

2. Establishment of an equation for critical feed rate that includes side flow angle groove parameters associate with side flow angle. According to the chip-breaking chart axes, chip-breaking occurs in a certain feed rate in a range of depth of cut that result side flow angle. Along side flow angle, equivalent groove parameters are defined that can be replaced with 2-D equations of critical feed rate and formulate a 3-D equation.

3. Analyzing chip breaking in precision machining. By the chip-breaking chart we can analyze extra chip breaking region that usually occurs in precision machining with protruded groove inserts.

Therefore the approach of present study is:

- Looking into details of relationship between chip-breaking chart and the insert groove parameters as well as cutting parameters
- After analysis, use experimental results to validate chip flow angle and groove details on chip formation and breaking.

3.3 Outline of Thesis

This section provides an overview of how the rest of the dissertation is organized.

Chapter 4 is formulation of influential parameters on 2-D and 3-D up-curl dominated chip. Through chip/insert geometric analysis, the original model of the chip-breaking limits is extended to include the backwall angle and a criterion to recognize the groove width and backwall height effectiveness. Theoretical critical feed rate are extended from 2-D to 3-D and the groove functionality limits are analyzed in this chapter.

Experiments are conducted to confirm the equations that are established and the results are compared with Zhou (2001-b) equations for chip radius.

Chapter 5 presents critical feed rate (f_{cr}) equation analysis for protruded type grooves. The chip-breaking limits (the maximum and minimum depth of cut) are first described and identified as functions of the insert geometric feature parameters. The effect of insert nose radius on chip thickness is also studied. The theoretical and semi-empirical chip-breaking models for 3-D protruded grooved inserts are established. Cutting tests are conducted to confirm the equations. The experiment-based approach is used for developing a chip-breaking prediction model.

Chapter 6 summarizes all work in this dissertation and describes the possible future directions in developing chip-breaking predictive models.

4 Influential Parameters on 2-D and 3-D Up-Curl Dominated Chip

In this chapter the existing equations of chip up curl radius (R_0) are first improved. Chip formation in 3-D groove studied and extended based on 2-D groove equations.

4.1 Influential Parameters on 2-D Up-Curl Chip

With regard to Equation (4-1) below the up-curl chip radius has a critical influence on the critical feed rate.

$$f_{cr} = \frac{\varepsilon_B}{\alpha_{ch}} \cdot \frac{C_h K_R R_0}{\sin \kappa_r} \tag{4-1}$$

where α_{ch} is cross-section shape coefficient, ε_B is tensile strain of the chip, R_0 is the chip up-curl radius, κ_r is the insert lead angle, C_h is the cutting ratio and K_R is the coefficient related to the chip radius breaking.

$$K_R = R_L / (R_L - R_0) \tag{2-14}$$

Past studies have been done mostly on chip radius in the 2-D groove (Zhou, 2001-b). In these papers, the backwall angle and backwall length to rake land length ratio are not considered.

In addition, insert makers have not identified the groove specifications in their catalogues. It is therefore difficult to identify the groove specifications and follow a track to model the grooves in chip formation process. The main objective of critical feed rate study is to establish a model for the up-curl chip radius equation, which shows groove specifications effect on chip radius dimension.

As explained in chapter 2 Zhou (2001-b) introduced the latest equation of chip up-curl (R_0). i.e.

$$R_o \approx \frac{W_n^{\,2} + h^2 + l_f^{\,2} + 2l_f\left(-W_n \cos\gamma_n + h\sin\gamma_n\right)}{2(W_n \cos\gamma_n + h\sin\gamma_n)} \qquad (4\text{-}2)$$

where W_n is groove width, l_f is the chip/insert contact length, γ_n is the rake angle in normal direction, and h is backwall height. In Equation (4-2) above when the backwall length (l_b) is longer than rake land length (l_n) (see Figure 4-1), the chip will leave the tool surface before reaching the backwall end.

Therefore, the overall length of the measured the backwall height and groove width cannot be substituted in Equation (4-2).

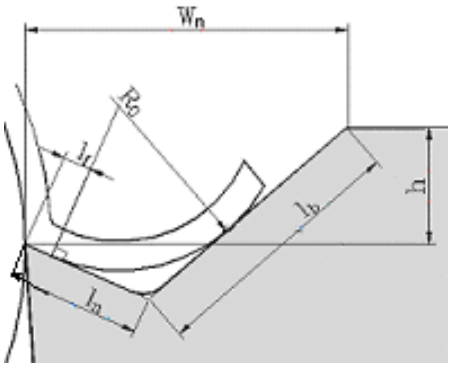

Figure 4-1 Chip Formation in Long Backwall Groove

However with regards to Figure 4-1 a new equation for R_0 is formulated (see below) for this research:

$$R_0 = \left(\frac{\left(W_n - h\cot\gamma_b - l_f\left(\frac{\tan\gamma_n}{\sin\gamma_b} + \cos\gamma_n\right)\right)}{\frac{\tan\gamma_n}{\sin\gamma_b} + \cos\gamma_n} \right) \tan\left(\frac{\gamma_n + \gamma_b}{2}\right) \qquad (4\text{-}3)$$

where γ_b is backwall angle. Equation (4-3) is such arranged that the measured W_n and h can be substituted directly. Equation (4-3) is functional when the following condition which is called *criterion equation*, is fulfilled:

$$\frac{l_b}{l_n - l_f} = \frac{\sin(\gamma_n + \beta)}{\sin(\gamma_b - \beta)} > 1 \tag{4-4}$$

where the l_b is rake face length, the l_n is backwall length and β is:

$$\beta = \arctan\left(\frac{l_f \tan\gamma_n + h}{W_n - l_f \cos\gamma_n}\right) \tag{4-5}$$

It should be considered that chip has a circular shape and it is tangent to chip groove wall in initial and final contact points of chip formation.

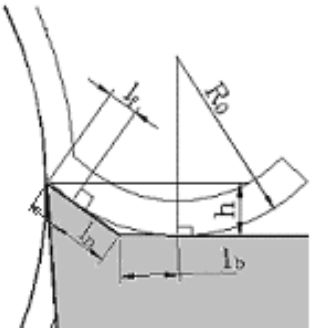

Figure 4-2 Chip Formation in Insert Without Backwall

Equation (4-3) cannot be used under the condition that the groove has no backwall, since there is no groove width as shown in Figure 4-2. Therefore Equation (4-6) is formulated to calculate the radius of chip curl as follows:

$$R_0 = \frac{\left(\frac{h}{\cos\gamma_n} - l_f(2\cos\gamma_n + \sin\gamma_n)\right)}{\cos\gamma_n} \tag{4-6}$$

In this section it is found that the nominal groove width and backwall height that are usually referred to as criteria for chip breaking are not always trustable and should be

categorized to models (Equation (2-4), (4-2), (4-3)) with respect to groove dimensions and section profile. In these equations, except (2-4), the only parameter that should be estimated from data base is the chip/insert contact length (l_f). It is, therefore recommended that instead of evaluating groove parameters individually, according to chip up-curl model the chip radii should be calculated and results compared.

4.2 Influential Parameters on 3-D Up-Curl Dominated Chip

According to the cutting tool classification defined in chapter 2, and with respect to Figure 4-3, the Equations (2-4), (4-3), (4-4) and (4-6) mentioned in chip radius modeling cannot be used in 3-D unless the groove specifications are considered along with the chip flow.

4.2.1 Chip Side Flow Angle (ψ_λ)

Rahman et al (1996) have studied chip formation in 3-D and formulated the groove specifications along chip flow. In this part his work is revised and chip formation equations are organized according to influential parameters including groove width, rake and backwall angle.

The Chip flow angle is a key parameter that determines the groove designs in 3-D. In this regard the chip side flow angles should be determined. The side flow angle depends on workpiece material, insert dimension specifications and machining conditions (Young 1987). This study takes account of the Colwell equations (Stabler 1964), because it covers all geometrical specifications of insert. Hence the chip side flow angle ψ_l equation is:

$$\psi_\lambda = \tan^{-1}\left(\frac{\sqrt{2r_\varepsilon d - d^2} + f/2}{d}\right) \qquad \frac{d}{r_\varepsilon} < (1-\cos\kappa_r) \qquad (4-7)$$

$$\psi_\lambda = \tan^{-1}\left(\frac{d/\tan\kappa_r + r_\varepsilon \tan(\kappa_r/2) + f/2}{d}\right) \qquad \frac{d}{r_\varepsilon} \geq (1-\cos\kappa_r) \qquad (4-8)$$

where r_ε is nose radius, d is depth of cut, κ_r insert lead angle and f is feed rate. As it can be seen in Stabler equations i.e. (4-7) (4-8) the most important parameters of insert that have influence on side flow angle are represented. It should be noted that r_ε is insert feature, f and d are machining conditions, κ_r is insert orientation that can be studied separately.

In orthogonal machining groove, nominal parameters were considered in the equations of chip formation because the chip flows perpendicular to groove on rake face. However in oblique machining in presence of side flow angle the groove nominal parameters will not be accurate and they should be considered along the chip flow direction. Therefore in order to calculate the chip up-curl accurately, it is required to consider groove parameters along side flow angle. The side flow angle equations for certain insert is also a function of machining conditions (depth of cut, feed rate) and it can be concluded that the groove parameters are a function of machining conditions and they change in different depths of cut and feed rates. The groove parameters along the chip flow are called equivalent parameters that are analyzed in detail in the next section.

4.2.2 Equivalent Parameters

With respect to side flow angle (ψ_λ), the groove parameters, influenced by side flow angle, as shown in Figure 4-3 are:

- **γ_{ne}: Equivalent Insert Rake Angle**
- **γ_{be}: Equivalent Groove Backwall Angle**
- **W_{ne}: Equivalent Groove Width**

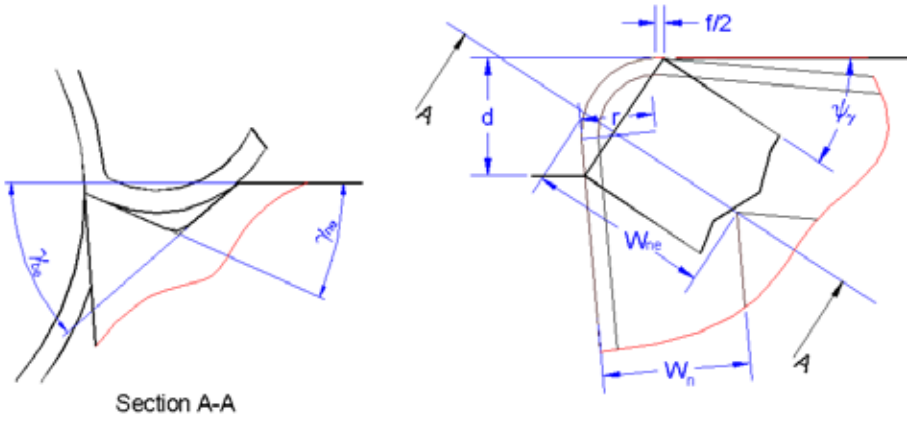

Figure 4-3 Equivalent Parameters along Chip Formation

Insert Equivalent Rake (γ_{ne}) and Backwall Angles (γ_{be})

The rake and backwall angle are altered with respect to chip side flow angle. The equation of the equivalent rake and backwall angle, in this case is given as:

$$\gamma_{ne} = \text{Arc}\tan\frac{\cos\psi_\lambda}{\cot\gamma_n} \tag{4-9}$$

$$\gamma_{be} = \text{Arc}\tan\frac{\cos\psi_\lambda}{\cot\gamma_b} \tag{4-10}$$

Insert Equivalent Groove Width (W_{ne})

In up curl dominated chip radius Equation (4-3), (4-4), and (4-6), the groove width is the most important parameter that affects chip radius dimension with respect to groove type, especially in simple grooves, can be significantly affected by chip side flow angle. In simple type of 3-D grooves Figure 4-4 the following equations govern the groove width dimension:

$$W_{ne} = r_\varepsilon - b_{\gamma 1} + \frac{W_n + b_{\gamma 1} - r_\varepsilon}{\sin(\psi_\lambda + \kappa_r)} \qquad \psi_{\lambda cr1} < \psi_\lambda \qquad (4-11)$$

$$W_{ne} = \frac{W_n - b_{\gamma 1}}{\sin(\psi_\lambda + \kappa_r)} \qquad \psi_{\lambda cr1} \geq \psi_\lambda \qquad (4-12)$$

where $b_{\gamma 1}$ is insert/chip restricted contact length.

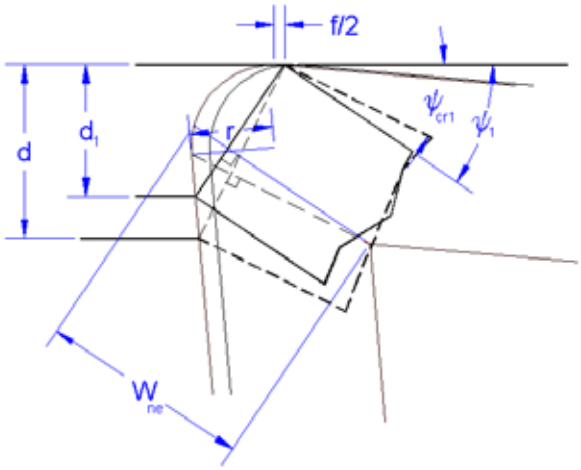

Figure 4-4 Chip Side Flow Angle ($\psi_{\lambda cr1}$) Indicates the Groove Width Equation Limit

In these equations if the insert has no insert/chip restricted contact length the $b_{\gamma 1}$=0.

Chip side flow angle ($\psi_{\lambda cr1}$) that shows the limitation of Equation (4-11) and (4-12) is based on minimum groove width along chip flow direction. This means that in the simple type 3-D grooves the chip is shaped in contact with the groove nose, Figure 4-4. Even when the depth of cut is greater than the insert nose radius, the minimum groove width along chip side flow angle is from groove nose to a point within insert nose radius, which can be calculated by Equation (4-13).

$$\psi_{\lambda cr1} = \cot^{-1}\left(\left(\frac{r_\varepsilon \sin\left(\frac{\alpha}{2}\right)}{(W_n - r_\varepsilon)\sin\left(\frac{\alpha}{2} + 2\kappa_r\right)} + \cot\left(\frac{\alpha}{2} + 2\kappa_r\right)\right) - \kappa_r \qquad (4-13)$$

where α is insert nose angle.

Since protruded grooves are usually used for finishing and the depth of cut is within insert nose radius, chip deals only with groove nose. Therefore the groove parameters are along the line that starts from groove nose to insert nose (see Fig 4-5).

The groove width in protruded groove inserts is very small and the chip side flow angle does not change significantly because of small depth of cut. Thus the equivalent groove width (W_{ne}) can be taken as equal to nominal groove width (W_n) i.e.

$$W_{ne} = W_n \tag{4-14}$$

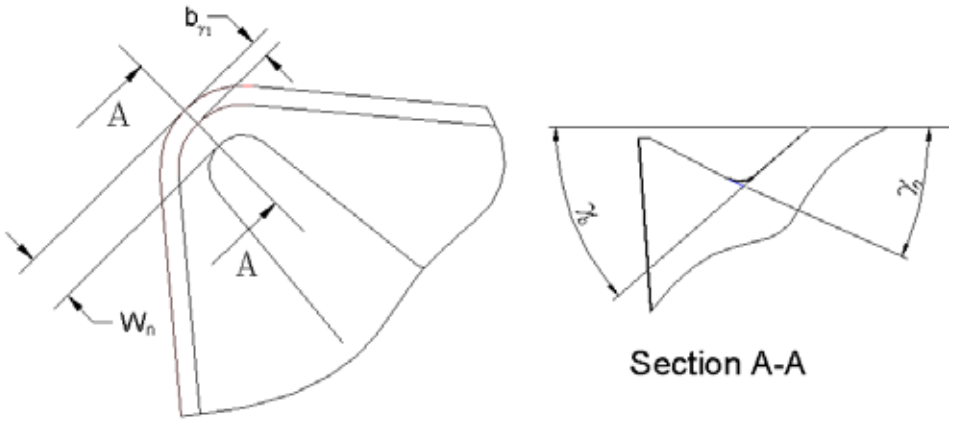

Figure 4-5 Groove Dimensions in Protruded Groove Type Inserts

Another limitation of chip side flow angle is angles that cause the chip does not reach the groove nose (see Figure 4-5).

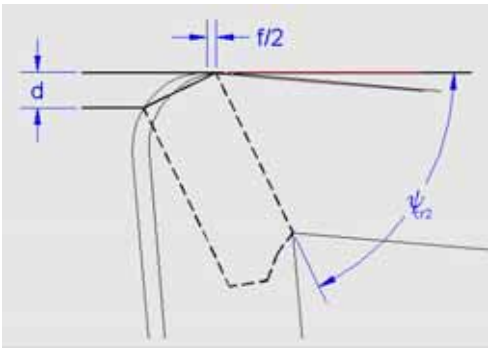

Figure 4-6 Groove Side Flow Angle Related to Effectiveness of Groove

For these cases the following equation is established as follow:

$$\psi_{\lambda cr2} = \frac{\left(\frac{w_n - r}{\cos(\frac{\alpha}{2} + \kappa_r)} + \sqrt{2}r\right)\sin\left(\frac{\alpha}{2} + \kappa\right)}{\left(\left(\frac{w_n - r}{\cos(\frac{\alpha}{2} + \kappa_r)} + \sqrt{2}r\right)\cos\left(\frac{\alpha}{2} + \kappa_r\right) - \frac{f}{2} - \sqrt{2}r\cos(\frac{\alpha}{2} + \kappa_r)\right)} \quad (4\text{-}15)$$

When the chip side flow angle is greater than critical side flow angle the chip is not curled by insert groove.

As discussed early in this chapter the critical feed rate Equation (4-1) chip radius is one of parameters that has important role and should be analyzed accurately. Therefore in order to maintain a comprehensive chip up curl radius equation, the up-curl chip equation first was improved and chip curling in the grooves which backwall length (l_b) is longer than rake land length (l_n) and grooves without backwall were established (Equation (4-3) (4-6)). To identify that l_b is longer than l_n Equation (4-4) as a criterion was formulated. If Equation (4-4) is greater than 1 Equation (4-3) can be used. However the chip radius equations are based on groove parameters in 2-D and chip side flow angle during chip flow and 3D grooves are not considered. Consequently groove parameters

(groove width (W_n), rake angle (γ_n), backwall angle (γ_b)) were formulated along with side flow angle (Equation (4-9), (4-10), (4-11), (4-12)) and called equivalent parameters (groove width (W_{ne}), rake angle (γ_{ne}), backwall angle (γ_{be})). Also the side flow angles ($\psi_{\lambda cr1}$) that identifies which equation of groove width should be implemented was established (Equation (4-13)). In Figure 4-15 the flow chart of calculation chip radius in 3-D are shown.

4.3 Experimental Validation

In order to validate Equation (4-3) and (4-4) as the criterion equation derived in this research work and analysis, the side flow angle effects (4-9 to 4-12) on the chip curl radius, the following test methodology was conducted:

- To measure chip diameter and compare it with estimated amounts.

In this step the estimated chip radius equations were compared with practical values and the equation that has accurate prediction was indicated.

- To determine the chip side flow angle effects on chip radius.

In this step to validate, if the chip radius could be predicted by the equations of chip radius with equivalent parameters, the produced chip radii in different side flow angles were compared with the prediction.

4.3.1 Experiment Design

To achieve the follow up goals, a longitudinal dry-cutting test with a manual lathe machine in the following machining conditions was conducted:

Table 4-1 Test Parameters for Machining

No.	Insert Type	W/P Material	Feed Rate (in/rev)	Depth of Cut (in)	Surface Speed (Sfpm)
1	TNMP 332K KC850	1010	0.0046	0.03	523
2	CNMG432-NL92	4150	0.011 0.015	0.03,0.05 0.06	169

In this experimental work two kinds of inserts, shown in Figure 4-7, were implemented as 3-D type groove inserts.

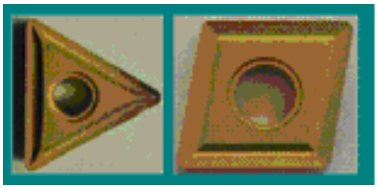

1)TNMP 332-KC850, 2)CNMG 432 NL92

Figure 4-7 Inserts Implemented in Experimental Validation

The measured parameters of these inserts were listed in Table (4-1). In this table the nose radius values were given by the inserts manufacturers. The CNMG432-NL92 insert is scanned in Surface Metrology Laboratory by UBM-Microfocus scanning laser profiler (see Figure 4-8); the profile software was used to produce and measure the insert profile in the specified section, Figure 4-9.

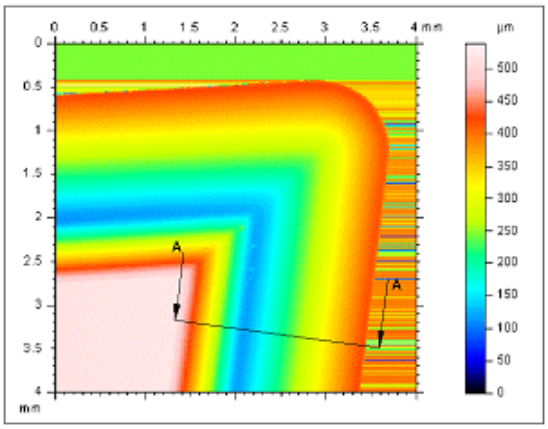

Figure 4-8 Scanned Picture of CNMG432-NL92 Insert

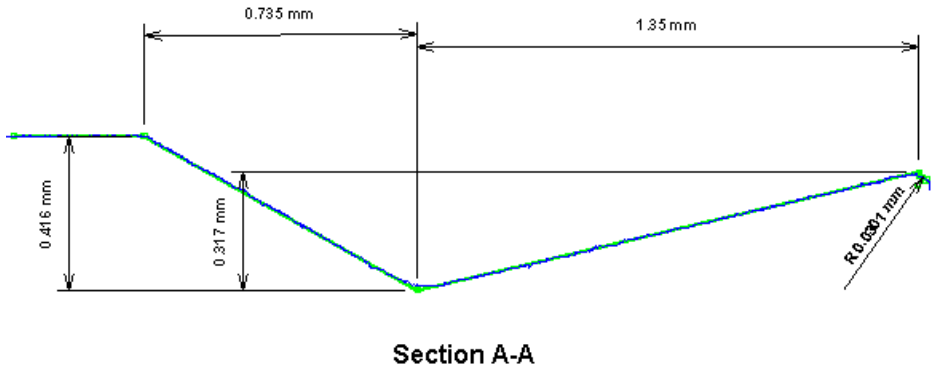

Figure 4-9 Dimensions of CNMG432-NL92 Insert along Section A-A

The rest of insert dimensions were extracted from Zhou's dissertation (Zhou 2001-b).

Table 4-2 Insert Measurement Results

No.	Insert Type	Manufacturer	r_ε (mm)	W_n (mm)	$b_{\gamma 0}$ (mm)	h (mm)	γ_n(°)	γ_b(°)	κ_r(°)
1	TNMP 332K KC850	Kennametal	0.80	2.7	0.025	0.18	10	10.2	90
2	CNMG432-NL92	Kennametal	0.80	2.1	0.03	0.1	13.2	29.5	95

To perform measurement of side flow angles and chips dimensions a digital Sony model MVC-FD91, with a shutter speed of 1/1000 second and flashlight was employed. Pictures were taken at a 1024*768 resolution with JPG extension files.

A base was made and placed in machining position to support the camera during machining. The camera was leveled above the machining position. Three pictures were taken in each step.

The pictures were transferred to AutoCAD software as a raster image to take measurements.

4.3.2 Experimental Results

To verify Equation (4-2) and (4-3) TNMP 332K KC850 insert was selected. By this insert 1010 steel was machined with 0.03 in depth of cut and 0.0046 in/rev feed rate (see Figure 4-10).

Figure 4-10 TNMP 332K KC850 Insert with 0.03 in. Depth of Cut 0.0046 in/rev Feed Rate

As shown in Figure 4-10 the produced chip is up-curl dominant and the chip radius is 1.9 mm. The chip radius is therefore calculated with Equations (4-2) and (4-3) (see Table 4-3).

Table 4-3 Calculated Results for TNMP 332K KC850 Insert

Insert	Machining Condition	W_{ne} (mm)	L_f (mm)	Criterion	R(Li) (mm)	R (Avan.) (mm)	R Measured (mm)
TNMP 332K KC850	0.03 DOC (in.) 0.0046 FR (in/rev)	2.7	0.55	5.81	5.96	1.89	1.9

In these equations all parameters were the same except l_f, which was estimated based on measured chip radius. As it can be seen in Table (4-3) the criterion is 5.81 mm which is far greater than 1. Therefore Equation (4-3) named *Avanessian model* is functional. Chip radius by Li's method was calculated and shows that the result was

greater than the measured radius. In Figure 4-11 the produced chip was modeled showing that the chip can not reach the groove end. With regard to dimensions it left before reaching groove backwall end.

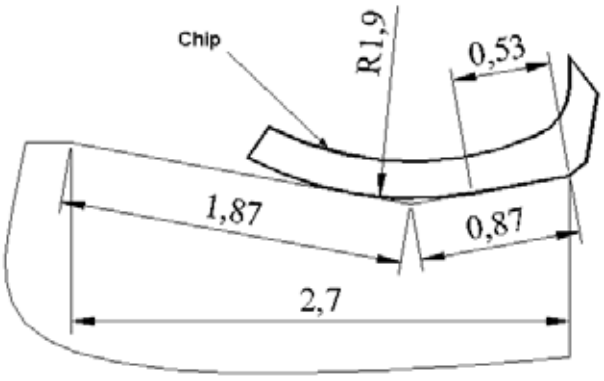

Figure 4-11 Produced Chip Situation on TNMP 332K KC850 Insert Groove

In finding the chip radius, as stated above, from analytical equations the only unknown parameter was the chip insert contact length (l_f). For example as it can be seen maximum contact length in Figure 4-11 is 0.87 mm. Therefore to prove that with different l_fs which varies between zero and the rake land length, it is not possible to calculate measured chip radius by Zhou's equation, the following graph was drawn (see Figure 4-12).

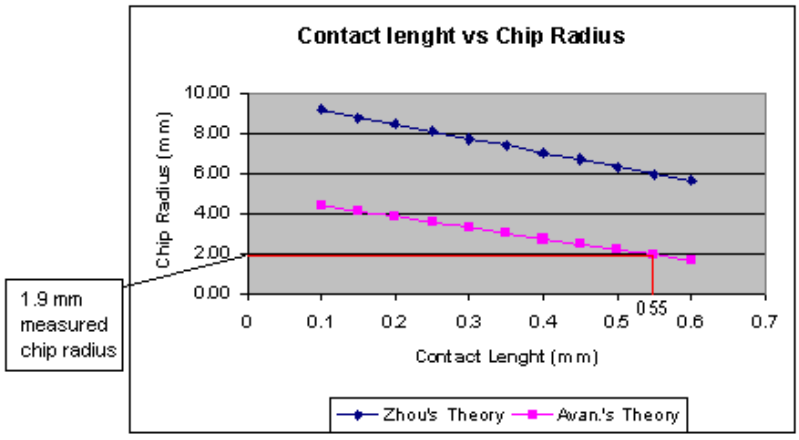

Figure 4-12 Comparison between Avanessian and Zhou's Models for Chip Radius Produced by TNMP 332K KC850 Insert

As it can be seen in Figure 4-12 the calculated chip radius with different l_f s in Zhous's model lie within 6 to 9mm which does not match with the measured chip radius i.e. 1.99. But in Avanessian's model with different l_fs, however, the radius of the chip was found at l_f=0.55mm which agrees with the calculated value in Table 4-3.

Chip Side Flow Angles Effects on Chip Formation

To analyze side flow angle effects on chip formation, as explained before, groove equivalent parameters (groove width (W_{ne}), rake angle (γ_{ne}), backwall angle (γ_{be})) should be first calculated. For this purpose CNMG432-NL92 insert was utilized and the following results were calculated as shown in Table 4-4.

In this Table and according to Equations (4-9), (4-10), (4-11) and (4-12) to calculate equivalent parameters the side flow angle should be estimated.

Insert	Machining Condition (in)	ψ_λ (^{o})	W_{ne} (mm)	γ_{ne} (^{o})	γ_{be} (^{o})	L_f (mm)	Criterion	R(Li) (mm)	R (Avan.) (mm)	R Measured (mm)
CNMG432 -NL92	0.03DOC 0.015 FR	45	2.82	9.4	21.8	0.8	1.04	4.96	3.60	3.65
	0.03DOC 0.011 FR	38	2.77	10.4	24.0	1.2	1.69	1.63	2.31	2.3
	0.05 DOC 0.011 FR	24	2.4	12.0	27.3	0.85	1.27	2.15	2.03	2.15
	0.06 DOC 0.011 FR	12	2.20	12.9	28.5	0.62	1.05	2.38	1.98	2.22

Table 4-4 Results of CNMG432-NL92 Inserts Machining

During machining, under the conditions mentioned in Table 4-4 above, pictures were taken and then side flow angles (ψ_λ) measured as shown in Appendix A. The same method was also used to measure the produced chips as shown in Appendix B.

Based on these measurements of side flow angles the groove equivalent parameters, including groove width (W_{ne}), rake angle (γ_{ne}) and backwall angle (γ_{be}) were

calculated. As it can be seen in Table 4-4 the smaller the side flow angle the smaller the groove width. However, a smaller side flow angle gives greater insert rake and backwall angles. In the table l_fs were estimated based on measured chip radii in table 4-4.

Despite our anticipation that by altering the side flow angle the chip radius should change, nonetheless, the measured chips radii (except for the first one) are almost equal. By analysis of the criterion number it can be seen that the smaller the side flow angle the smaller the chip/insert contact length which means that the bigger effective groove width is involved in chip formation.

Also it can be seen that because the criterion number is close to one there is not a big difference between Avanessian's and Zhous's models.

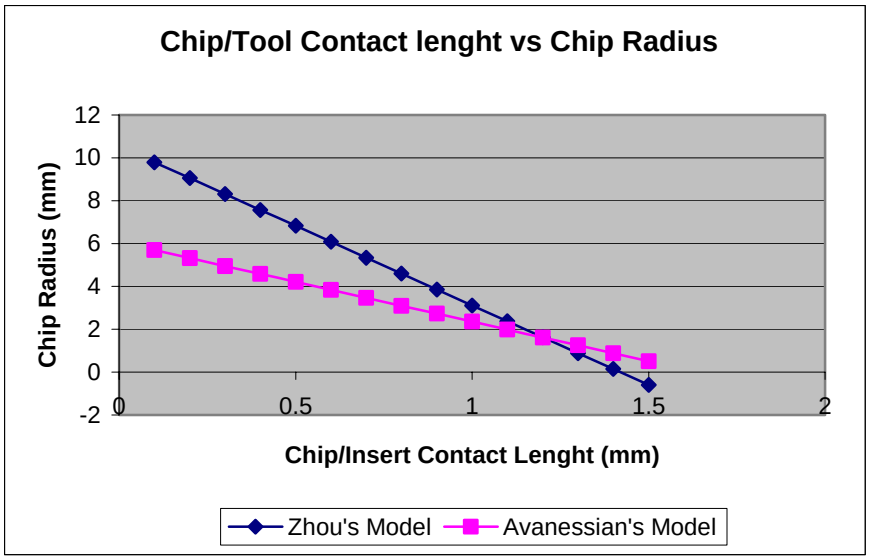

Figure 4-13 Comparison between Avanessian and Zhou's Models for Chip Radius Produced by CNMG432-NL92 Insert

In Figure 4-13 the chip radius was plotted against corresponding insert/chip contact length for the 38° side flow angle. As we can see unlike Figure 4-12 the predicted chip radius, at l_f=1.2 mm, is very close. By subtle changes in the l_f the required chip radius 2.3 mm can be obtained in both models.

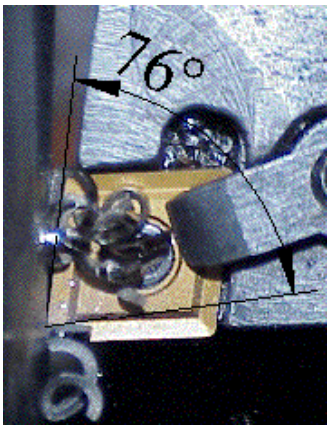

Figure 4-14 Side Flow Angle in 0.015 in/rev Feed Rate and 0.017 in. Depth of Cut

Figure 4-14 shows that the chip side flow angle is greater than the determinative angle. Consequently, the chip is formed without reaching insert groove backwall.

The flow chart/algorithm (Figure 4-15) shows the process of calculating the chip radius.

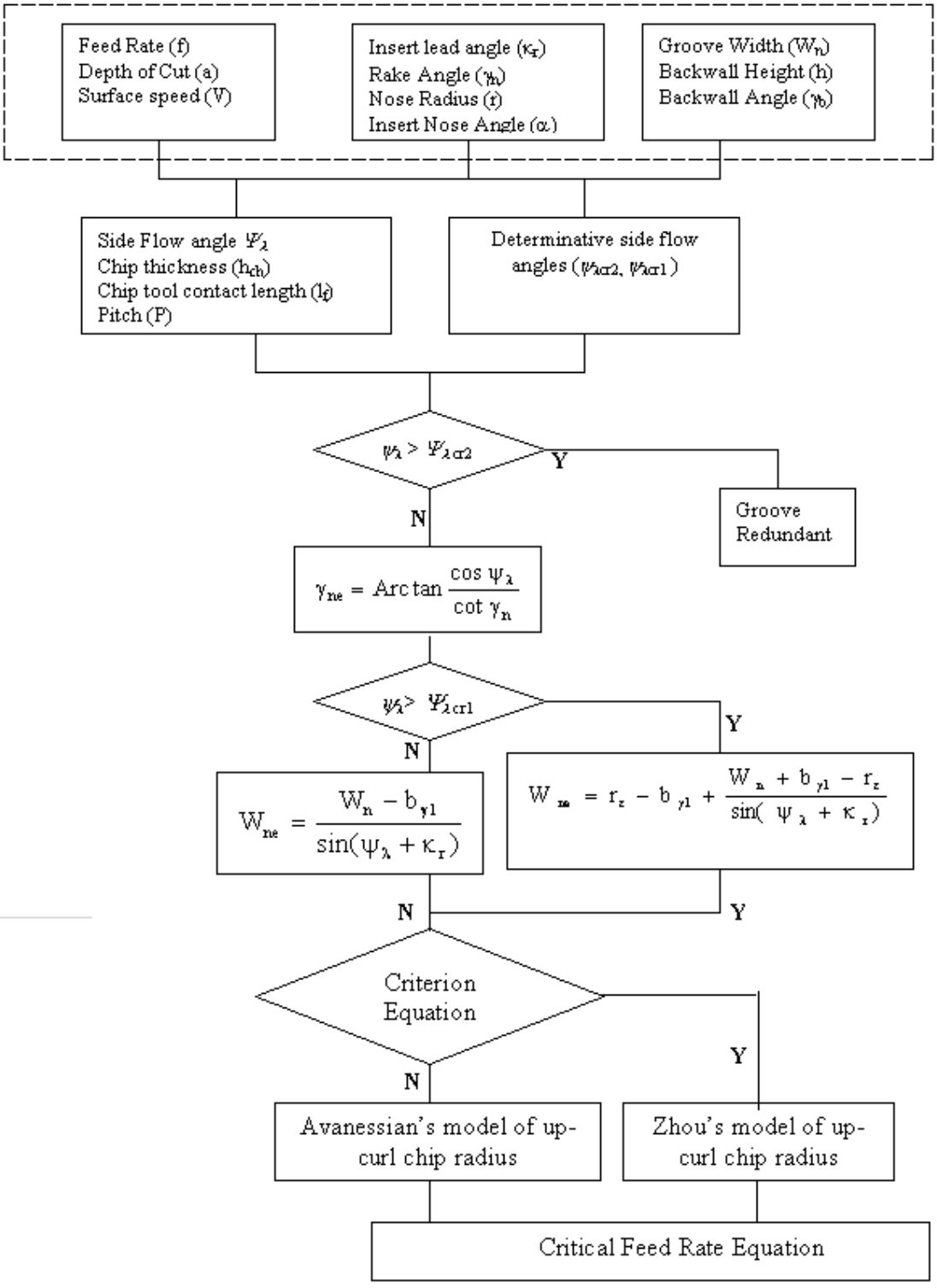

Figure 4-15 Flow Chart of Influential Parameters on Up-Curl Chip

4.4 Summary

In this chapter the theories and equations of chip formation in grooves were reviewed. Also chip formation in 2-D groove was improved and chip formation in 3-D groove is studied. At the end, some experiments were conducted to verify the theoretical equations. The work done in this section therefore includes three parts:

1. Improvement of chip up curl radius for insert with long backwall.

According to the review the Equation ($R_0 = R$) covers the cases that the section profile of groove was a portion of curve. In conditions that the chip does not follow the groove section profile or the section profile was V type the Zhou's Equation (4-2) was implemented. But Zhou's equation does not cover conditions that the backwall length is longer than the rake face length, so according to Nakayama et al assumption Equation (4-3) was formulated. The Equation (4-3) was functional when Equation (4-4) was fulfilled.

Equation (4-3) cannot be used under conditions that the groove has no backwall. Thus Equation (4-6) was established to calculate radius of chip curl.

2. Improvement of up-curl chip radius from 2-D to 3-D.

As mentioned in the beginning of this section all of these equations were formulated for orthogonal cutting in 2-D space that was not match with real machining circumstances, which the groove is 3-D. Groove equivalent rake ($\mathbf{g}_{ne}$) and backwall angles ($\mathbf{g}_{be}$) and width (W_{ne}) were considered in 3-D formation of chip and formulated in Equation, (4-9) to (4-12). Also the side flow angle ($\psi_{\lambda cr1}$) was indicated in Equation (4-13) that identified which equation of groove width should be implemented was formulated.

In protruded grooves the nominal groove width is the distance of insert nose to the middle of the groove nose. The equivalent groove width is equal to nominal groove width i.e. $W_{ne} = W_n$

From the above analysis of chip breaking critical feed rate equation the following conclusion can be made.

3. Verification of the derived radius equations and side flow angles effects on chip radius.

The experimental work for insert verified the Avanessian's and Zhou's models. Also, the side flow angle effects on chip radius shows that chip radius was constant and did not affect chip formation since a combination of effective chip groove width, chip/tool contact length and groove equivalent parameters were involved in chip formation. Groove width increases because of side flow angle, which could cause chip/insert contact length to increase. The effective groove width reduction caused the chip radius to remain constant in different side flow angles.

5 Critical Feed Rate Equation Analysis with Protruded Type Grooves

In the previous chapter the side flow angle effects on chip formation were analyzed and a new concept was concluded about the insert parameters associated with the chip side flow angle. By this concept, protruded groove inserts and related extra chip-breaking region, introduced in Chapter 1, can be studied. Therefore in this chapter the critical feed rate equation and constrains in protruded type inserts is analyzed.

5.1 Limits of Extra Chip Breaking Region

To find out the limits of critical feed rate within the extra chip-breaking region, the limits of depth of cut in the region should be identified. The estimation of the depth of cut limits including the minimum depth of cut where depth of cut greater than that the chip breaks at the beginning of extra chip-breaking region and maximum depth of cut where greater than that the chip does not break at the end of extra chip-breaking region are hereby investigated.

5.1.1 Minimum Depth of Cut (d_{min})

In order to find the minimum depth of cut, hence the minimum chip curl, the minimum groove width is taken as principal.

With regard to Figure 5-1 and chapter two the minimum groove width in protruded groove inserts is along the symmetric line that goes through the insert nose. Thus the minimum depth of cut will be the point where the symmetric line meets the insert nose radius. The equation below summarizes the discussion on minimum depth of cut.

$$d_{min} = r_\varepsilon - r_\varepsilon \cos(\kappa_r + \frac{\alpha}{2}) \quad (5\text{-}1)$$

where α is insert nose angle and $r\varepsilon$ is nose radius.

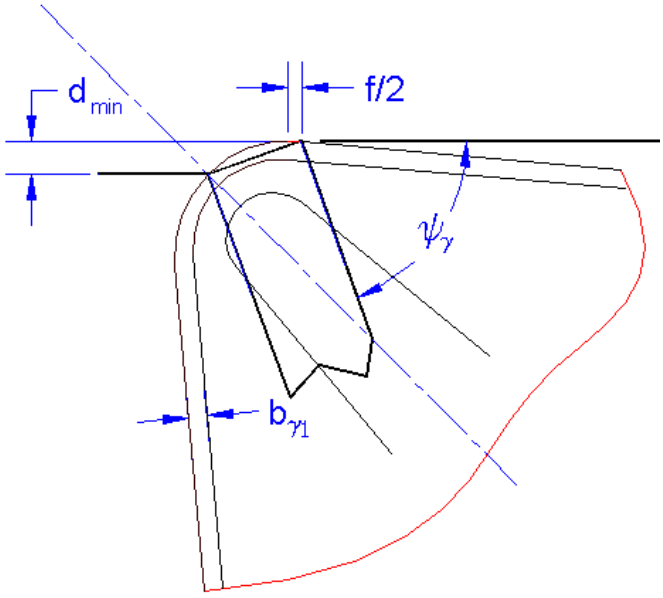

Figure 5-1 Minimum Depth of Cut

5.1.2 Maximum Depth of Cut (d_{max})

The next phenomenon considered as ineffective groove or maximum depth of cut is the situation where the chip will not go through the groove properly. In this situation, as shown in Figure 5-2, initially the chip is separated from the workpiece in the insert

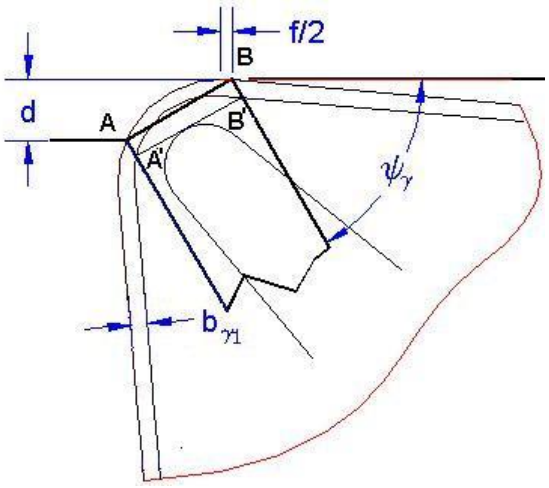

Figure 5-2 Machining Condition Where Groove is Ineffective

nose but in point A and B it is still attached to the workpiece. The chip blades in A and B then slide on insert restricted rake face and in points A' and B' where all section of chip are to go into groove, the chip-middle reaches the groove nose making it impossible for the chip to enter in the groove. Only the groove nose makes a curve on the chip surface.

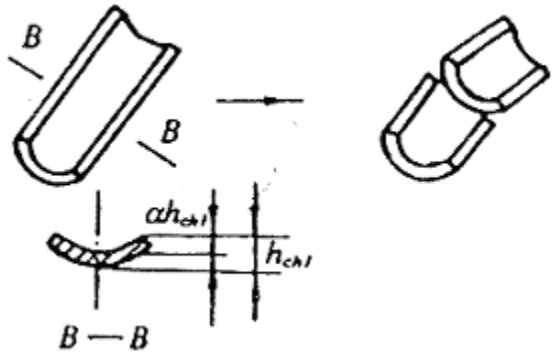

Figure 5-3 Chip Section Curved Due to Groove Nose Radius (Li, 1996)

This fact is more noticeable in grooves with zero or negligible backwall height.

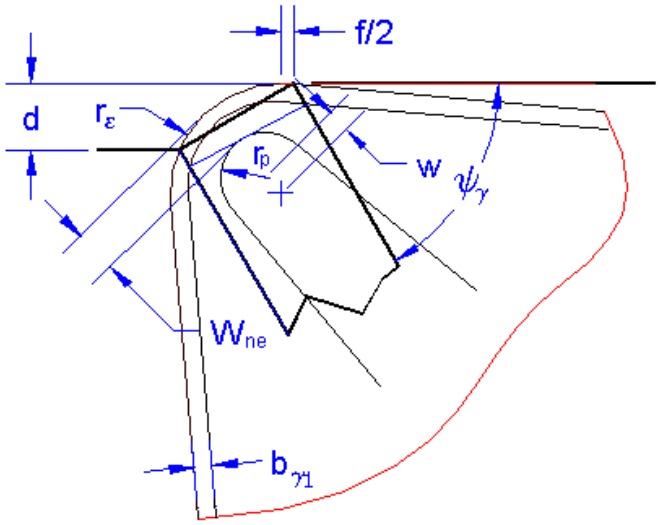

Figure 5-4 Maximum Depth of Cut

According to the above description and Figure 5-3, which shows influential parameters, the equation to estimate maximum depth of cut is established as follows:

$$d_{max} = 2\sqrt{r_\varepsilon^2 - (r_p + w)^2}.\sin\theta \tag{5-2}$$

where:

$$\sin\theta = \left(\frac{-b + \sqrt{b^2 - 4ac}}{2a}\right) \tag{5-3}$$

$$\begin{cases} a = y^2 + x^2 \\ b = 2.r_p.y \\ c = r_p^2 - x^2 \end{cases} \tag{5-4}$$

r_p is protruded nose radius

$$\begin{cases} x = \left(\frac{f}{2} + w + r_p\right)\sin(\kappa_r - \frac{\alpha}{2}) + b_{\gamma 1} \\ y = r_\varepsilon - w.\sin(\kappa_r - \frac{\alpha}{2}) - b_{\gamma 1} \end{cases} \quad (5\text{-}5)$$

w is the distance of the center of the protruded nose circle from insert nose radius center along insert symmetrical line. Since feed rate is small with respect to depth of cut, Equation (5-2) is neglected. This phenomenon has a more significant role in protruded type inserts with big nose radius.

For protruded groove where the groove nose sharp r_p is zero in Equation (5-2).

5.2 Nose Radius Effects on Chip Thickness

In protruded type inserts that are used mostly for finishing, the depth of cut usually is small. Therefore the uncut chip thickness is considered along the nose radius as shown in Figure 5-4. Chip thickness varies with constant feed rate and decreases significantly with reduction of depth of cut especially in inserts with great nose radius.

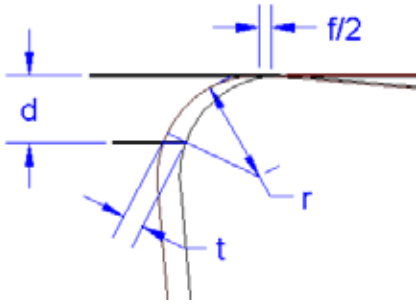

Figure 5-5 Uncut Chip Thickness in Small Depth of Cut

Therefore the Equation that is used to estimate chip thickness in round inserts can be implemented to calculate the uncut chip thickness on condition that the depth of cut is small.

From the discussion above the chip thickness in different depth of cut can be calculated using the following equations,

$$h_{ch} = \frac{f.\sqrt{\frac{2d}{r_\varepsilon} - \left(\frac{d}{r_\varepsilon}\right)^2}}{C_h} \qquad \frac{d}{r_\varepsilon} < (1 - \cos\kappa_r) \tag{5-5}$$

$$h_{ch} = \frac{f.\sin\kappa_r}{C_h} \qquad \frac{d}{r_\varepsilon} > (1 - \cos\kappa_r) \tag{5-6}$$

where;

κ_r is insert lead angle, C_h is ratio of uncut chip to chip thickness, r_ε is insert nose radius and f is feed rate.

To better understand the influence of depth of cut on chip thickness in Figure 5-6 three insert nose radii (0.047, 0.032, 0.015 in) were selected. These insert nose radii are standards in inserts dimensions and often implemented in machining.

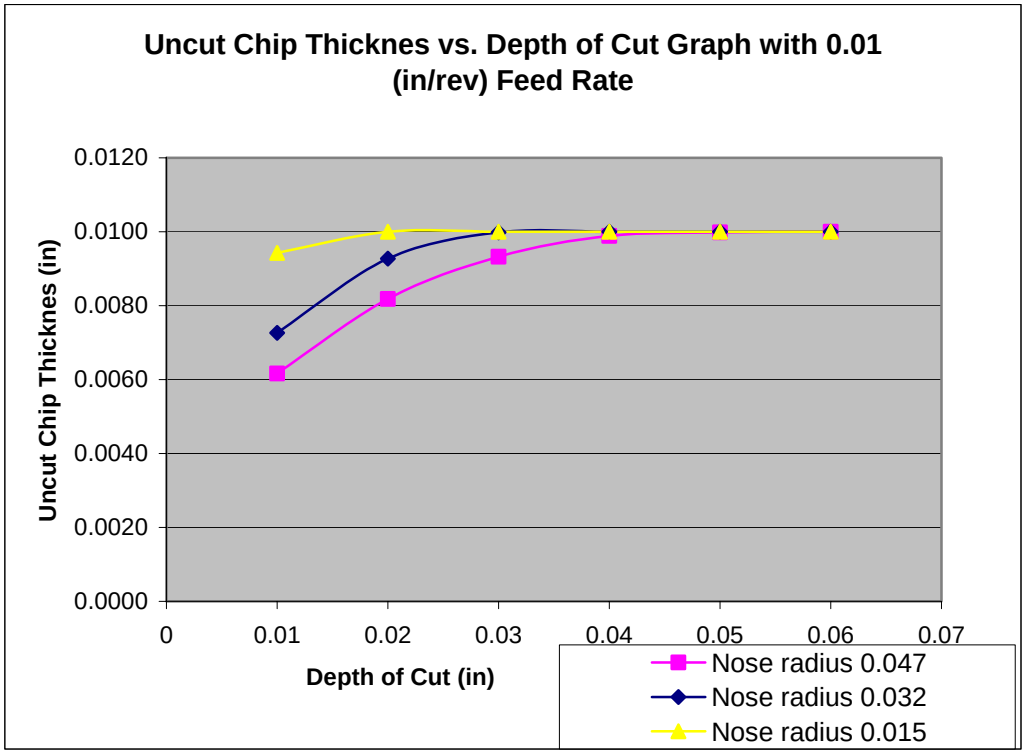

Figure 5-6 Uncut Chip Thickness Produced by Insert with Different Nose Radii with Different Depths of Cut

As it can be seen in Figure 5-6 the greater the nose radius the greater the effects of the depth of cut on the chip thickness.

With regard to conducted analyses, the analytical and semi-empirical critical feed rate equations are reviewed in the next section.

5.3 Analysis of Critical Feed Rate

In the introduction of this research work the Li and Zhou's works on chip breaking chart and critical feed rate, analytical and semi-empirical chip-breaking models were explained in detail (Zhou 2001-b). In this section the equations with new findings are improved and a new approach found for critical feed rate.

5.3.1 Theoretical Analysis of Critical Feed Rate

In chapter 4 equivalent parameters of groove were discussed. Also in section 5.1 both minimum and maximum depths of cut were discussed. Following these discussions and the nose radius effects on chip thickness, the equations below were formulated for critical feed rate in this research work:

$$f_{cr} = \frac{\varepsilon_b}{\alpha_{ch}} . \frac{C_h K_R R_0}{\sqrt{\frac{2d_{max}}{r_\varepsilon} - \left(\frac{d_{max}}{r_\varepsilon}\right)^2}} \qquad \frac{d}{r_\varepsilon} < (1 - \cos\kappa_\gamma) \tag{5-6}$$

$$f_{cr} = \frac{\varepsilon_b}{\alpha_{ch}} . \frac{C_h K_R R_0}{\sin\kappa_r} \qquad \frac{d}{r_\varepsilon} < (1 - \cos\kappa_\gamma) \tag{5-7}$$

In these equations it should be considered that the R_0, which is the up-curl chip radius can be substituted with any models of chip radius as explained in section 4.1. The model parameters can also be substituted for equivalent parameters as it was explained in chapter 4.

In protruded groove type inserts the minimum depth of cut stated in section 5.1.1 can be considered as the critical depth of cut i.e.

$$d_{cr} = r_\varepsilon - r_\varepsilon \cos(\kappa_r + \frac{\alpha}{2}) \tag{5-8}$$

Therefore we can say that the Equation (5-6) and (5-7) are theoretical critical feed rate equations in 3-D.

5.3.2 Semi-Empirical Chip-Breaking Predictive Model

As explained in chapter 2 another method of prediction of chip breaking is the semi-empirical chip-breaking model, which is a useful method to avoid extreme complexity of the chip-breaking. The critical feed rate equation as stated in chapter 2 is:

$$f_{cr} = f_0 K_{ft} K_{fV} K_{fm} \tag{5-9}$$

where f_0 is the standard critical feed rate under a predefined standard cutting condition. The predefined standard cutting condition can be any cutting condition. K_{fT} is the cutting tool (inserts) effect coefficient; K_{fV} is the cutting speed effect coefficient; and K_{fm} is the work-piece material effect coefficient.

In Zhou's work for the cutting tool (inserts) effect coefficient (K_{fT}) a linear combination of tool parameters (groove width (W_{ne}), rake angle (γ_{ne}) and backwall angle (γ_{be})) are used (Zhou 2001-b). But with regard to Equations (5-6) and (5-7) all parameters that expose insert parameters can be considered as K_{fT} and the rest K_{fm}.

Therefore the semi empirical equation with new definition for depth of cut greater and less than nose radius is:

$$f_{cr} = K_{fv} K_{fm} \cdot \frac{R_0}{\sqrt{\frac{2d_{max}}{r_\varepsilon} - \left(\frac{d_{max}}{r_\varepsilon}\right)^2}} \qquad \frac{d}{r_\varepsilon} < (1 - \cos\kappa_\gamma) \tag{5-10}$$

$$f_{cr} = K_{fv} K_{fm} \cdot \frac{R_0}{\sin\kappa_r} \qquad \frac{d}{r_\varepsilon} > (1 - \cos\kappa_\gamma) \tag{5-11}$$

The only parameter that is unknown in R_0 is l_f which according to Zhou's work in critical feed rate chip breaking point it can be substituted with a fraction of groove width.

Some experiments were conducted, as outlined in the following sections, in order to validate the equations discussed above.

5.4 Experimental Validation

In order to validate Equation (5-1), (5-2) and (5-5) for minimum and maximum depth of cut and chip thickness variation in small depth of cut derived in this research, work, respectively, chip-breaking charts were made by protruded groove inserts. In these charts, the minimum and maximum depth of cut were identified. Also chips thickness variations in constant feed rate with different depth of cuts were measured. Finally the results were compared with estimated values.

5.4.1 Design of The Experiments

To achieve the follow up goals a longitudinal dry-cutting test with a manual lathe machine in the following machining conditions was conducted:

- Workpiece material: 1010 steel
- Workpiece diameter: 3.850 in
- Surface speed: 520 sfpm

To carry out machining, four inserts with MTANR-12-3 tool holder were selected to be utilized as shown in Figure 5-7.

1)TNMG 333 QF 2)TNMG 332 QF 3)TNMG 333 QF 4)TNMG 332K

Figure 5-7 Protruded Grooves Inserts Implemented in Experiment

The inserts feature dimensions are listed in Table 5-1. Among all six parameters listed in Table 1-5, below, only the value of the insert nose radius was available from the insert manufacturers. The other parameters in the table were measured.

Table 5-1 Insert Geometric Parameters

No.	Insert Type	Manufacturer	r_ε (in)	r_p (in)	w (in)	$b_{\gamma 0}$(in)	γ_0(°)	γ_n(°)
1	TNMG QF 333 4025	Sandvik	0.047	0.008	0.019	0.004	15.0	14.7
2	TNMG QF 332 4025	Sandvik	0.031	0.007	0.01	0.008	16.6	19.3
3	TNMG QF 331 4025	Sandvik	0.015	0.003	0.006	0.007	11.9	20
4	TNMG 332K KC850	Kennametal	0.031	0.001	0.01	0.012	16.6	10.2

5.4.2 Experimental Results

The cutting tests results are listed in Table 5-2 from figures in Appendix C. In Table 5-2 the estimated amounts have enough accuracy to find the range of depth of cut where the groove is effective.

Also in this table, as expected, the greater the nose radius the greater the minimum depth of cut. However the maximum depth of cut does not follow only the nose radius dimension. Other parameters have their influences and are to be considered. Although, for example, in TNMG 33X QF insert sets (X=1,2,3) the greater the nose radius the greater the maximum depth of cut. The TNMG 332 K (with nose radius equal to the TNMG 332QF insert) the maximum depth of cut is greater than TNMG 333QF.

Table 5-2 Cutting Test Result

Insert	Minimum Depth of Cut (inch)		Maximum Depth of Cut (inch)	
	Estimated	Experimental	Estimated	Experimental
TNMG333QF	0.024	0.03	0.044	0.04
TNMG332QF	0.016	0.02	0.035	0.03
TNMG331QF	0.008	N/A	0.022	N/A
TNMG332K	0.016	0.02	0.052	0.05

In Figure 5-8 below the condition that the chip cannot enter into the groove is shown, including the position of the insert nose and the groove nose. In the time that the chip in point A and B was blocked by the insert blades the center of chip section that goes through A and B reached to the groove and has no room to enter into the groove. Only the curve as a mark made by the groove nose can be seen on the chip surface.

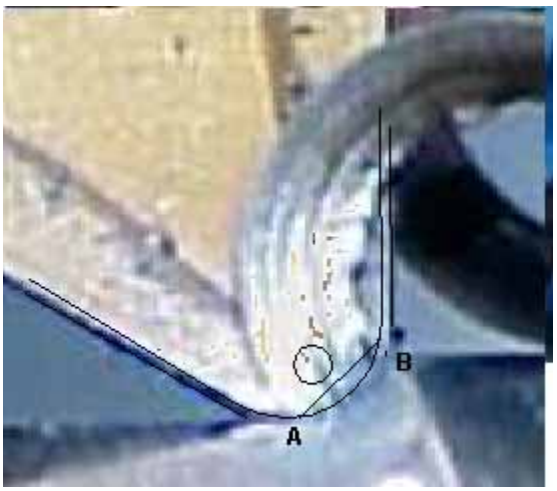

Figure 5-8 Chip Formation in 0.05 in. Depth of Cut 0.0056 in/rev Feed Rate

To better understand the differences between chip-breaking charts in simple groove insert and protruded groove insert, the chip-breaking chart of TNMG332 QF insert were studied in detail, Figure 5-9.

In the normal chip breaking-chart, the critical feed rate and depth of cut are unique. But as considered in chip breaking-charts of protruded grooves inserts, there is an extra area of broken chip. In Figure 5-9 the extra region of broken chip was identified by a boundary. As it can be seen this region does not follow the definition of critical feed rate and depth of cut, stated by Li (1990). Another difference between these charts is chip form. In the normal chip-breaking chart the chip in the critical depth of cut is side curl.

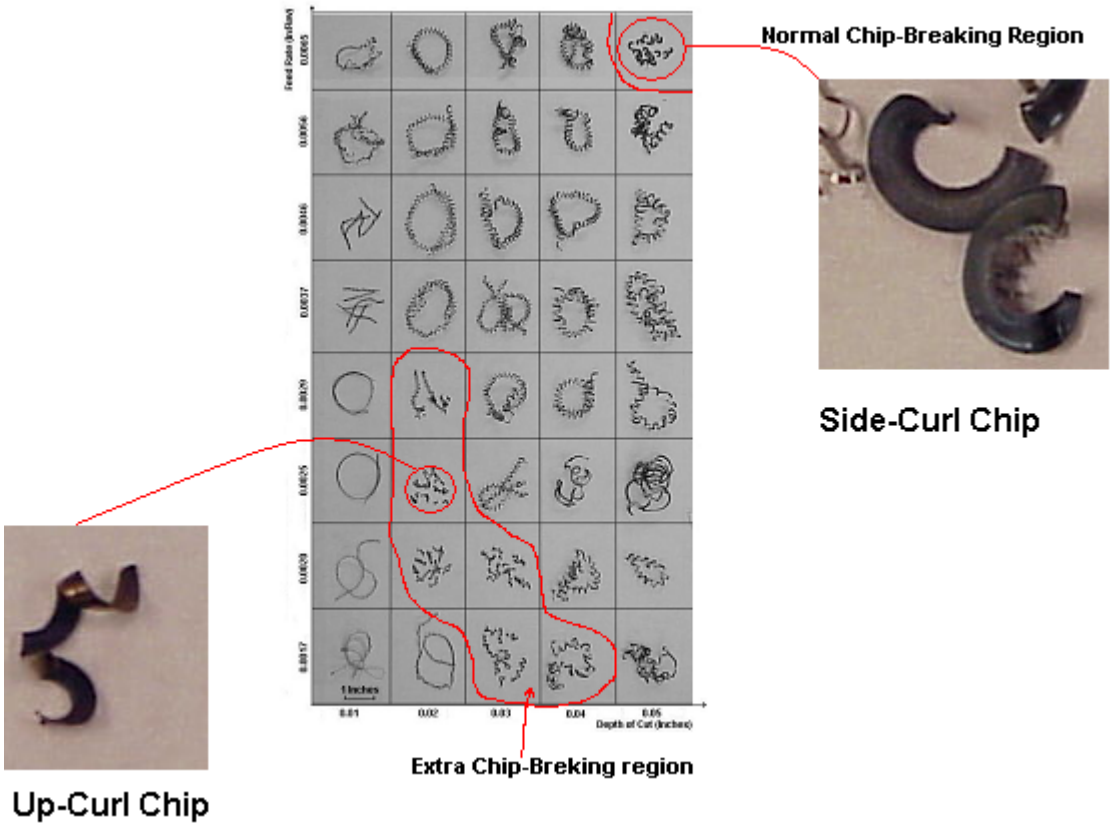

Figure 5-9 Chip Form in Different conditions of Chip-Breaking Chart Produced by TNMG 332-QF 4025 Insert

However, with respect to Figure 5-9 the chip that is magnified from 0.02 in depth of cut and 0.0025 in/rev feed rate point, the chip form is up-curl. In fact the region chips

that were supposed to be snarling chip formed as up-curl chip where there was a narrow groove.

Beyond this boundary, the chip cannot enter the groove. In ordinary chip-breaking region, shown in Figure 5-9, the chip is side-curl and the groove nose just made a curve or mark on the body of chip and has no direct role in chip formation.

To validate the effects of nose radius on chip thickness TNMG 333 QF insert was selected because of a big nose radius. As can be seen in Figure 5-10 chip thickness changes with depth of cut and becomes constant in depth of cut above the nose radius (nose radius for this insert is 0.047 in). Another phenomenon that was identified in Figure 5-10 is the effect of nose radius, which is insignificant on small feed rate.

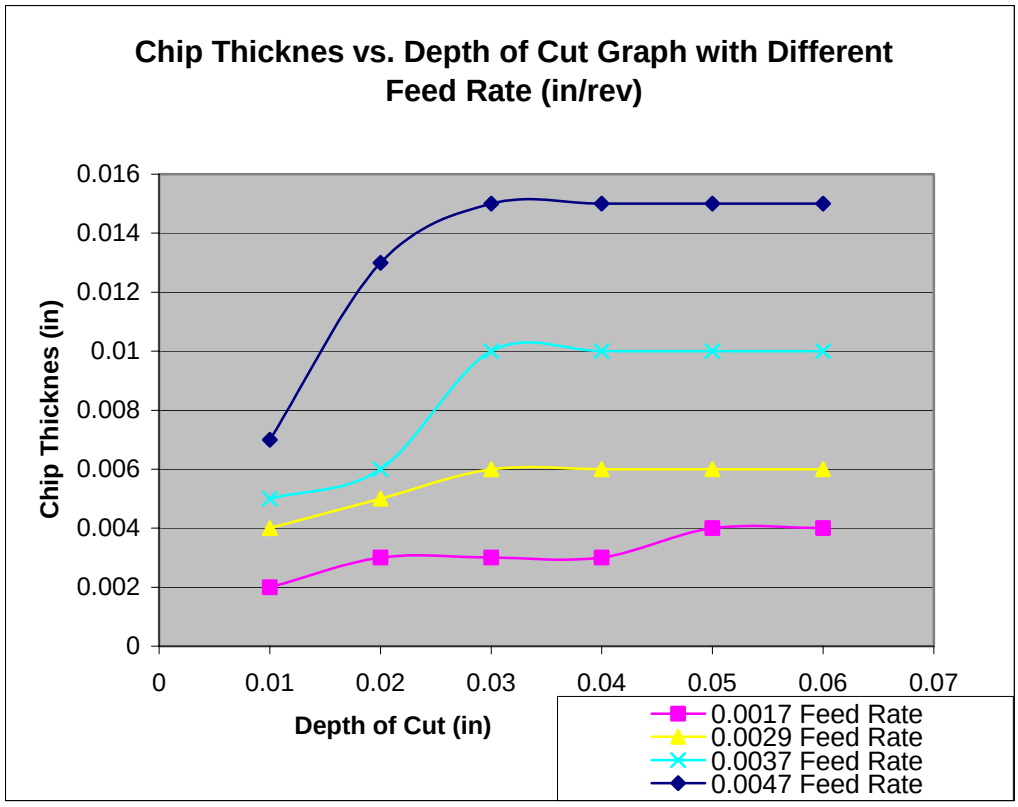

Figure 5-10 Chip Thickness in Different Depths of Cut Produced by TNMG 333-QF Insert with Different Feed Rates

It can therefore be concluded that in small depth of cut, according to Nakayama chip breaking criterion, the chip thickness is one of the parameters that has role in chip breaking. So that with small depths of cut and corresponding chip thickness the chip is unlikely to break.

In Figure 5-11 the chip thickness produced by inserts with different nose radius are compared. With respect to the curves, again the insert with greater nose radius has more effect on chip thickness in different depths of cut. But the inserts with 0.031 in and 0.015 in radii, there is not a great difference. The reason can be the effect of groove nose radius on chip thickness, which scratches or makes a curve on the chip.

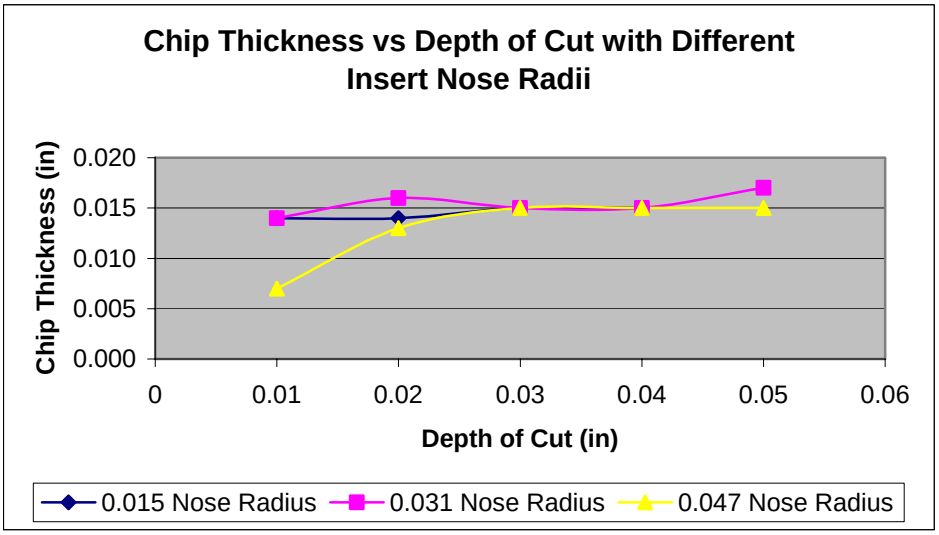

Figure 5-11 Chip Thickness in Different Depth of Cut Produced by TNMG 33x-QF Set Inserts with 0.0056 in/rev Feed Rate

5.5 Summary

In this chapter the limits of chip breaking chart for protruded inserts and the nature of broken chip were analyzed. It includes four parts:

1. Formulation of minimum and maximum depth of cut. The chip breaking limits in protruded type inserts that include maximum and minimum depth of cut were formulated in Equation (5-1) and (5-2). In these equations the maximum and minimum depth of cut could be calculated by only using insert parameters. In Equation (5-2) if groove nose was sharp then r_p is zero.

2. Chip thickness variations in small depth of cuts. When the depth of cut was small, the chip thickness varies, even though the feed rate was constant. In this chapter this variation was identified and formulated. The chip thickness could be calculated by Equation (5-5).

3. Critical feed rate improvement. Consequently the critical feed rate model was expanded to machining conditions where the depth of cut was small.

Related to critical feed rate for protruded groove inserts critical depth of cut was formulated by using minimum depth of cut Equation (5-8).

Also, a new approach was mapped out to predict chip breaking critical feed rate by semi empirical Equation (5-10) and (5-11) which were introduced for both greater and less than insert nose radii.

4. Validation of minimum and maximum depth of cut and chip thickness variation in different depths of cut. In the chart-breaking chart made by protruded groove inserts, an extra chip-breaking region was identified where the chips were up-curl and broken because of narrow groove, unlike the normal chip-breaking chart in which the critical depth of cut of the broken chip had side-curl. Finally the chip thickness variation in small depth of cut was validated and it was found out that in small depth of cut increasing feed rate had subtle effects on chip thickness as shown in Figure 5-10.

6 Conclusion and Future Work

6.1 Summary of this Research

Quality, productivity, cost, and environment are four main concerns in machining. Chip control has a very important role in achieving these concerns. To achieve the chip control goals in industry, developing and implementing chip-breaking predictive tools are crucial. The semi-empirical approach can be a powerful way to reach that goal. It bridges the existing gap between theoretical work on chip-breaking prediction and industrial requirements. The chip-breaking limits theory is the basis of the semi-empirical approach.

However, before utilizing the predictive models of the chip-breaking, the theoretical equations should be improved and extended from 2-D to 3-D. Also the limitations of theory, which are considered in this research, should be identified.

The main contributions in this research include:

1. The parameters that have influence on the chip formation were first analyzed in detail on critical feed rate model in the 2-D groove.
2. Establishment of an equation of critical feed rate that includes side flow angle and groove parameters associated with side flow angle.

According to the chip-breaking chart, chip breaking occurs in certain range of feed rates and depths of cut that results in side flow angle. Along side flow angle, equivalent groove parameters are defined that can be substituted into 2-D equations of critical feed rate to produce a 3-D equation.

3. For precision machining the chip-breaking chart was analyzed.

In the chip-breaking chart, the extra chip-breaking region that usually occurs in precision machining (small depth of cut and feed rate) with protruded groove inserts was analyzed. The chip-breaking application range (the maximum and minimum depth of cut) are first described and identified as functions of the insert geometric feature parameters. The effect of insert nose radius on chip thickness was also studied. The theoretical and semi-empirical chip-breaking model for 3-D protruded groove inserts was then formulated. Cutting tests were conducted to validate the equations.

6.2 Future Work

The inserts can be classified into four categories: inserts with a 2-D chip-breaking groove, inserts with a simple 3-D chip-breaking groove, inserts with a block-type chip breaker, and inserts with complicated geometric modifications. The theoretical and semi-empirical chip-breaking models extended in this research cover 3-D groove inserts especially insert with the protruded type groove. Future research may be conducted to develop chip-breaking predictive models for the other categories of inserts including a block-type chip breaker and those with complicated geometry modifications.

6.2.1 Inserts with Block-Type Chip Breaker

Inserts with a block-type chip breaker, especially cubic boron nitride (PCB) inserts, are widely applied in the soft-metal (e.g. copper, aluminum) cutting industry. For these inserts the process of developing a semi-empirical chip-breaking predictive model can be similar to the process for modeling 3-D grooved inserts. The first step in this process is the definition and measurement of insert / breaker geometric features. The second step is carrying out cutting tests, followed by modeling work and model

validation. Figure 6-1 shows the geometric features of inserts with a block-type chip breaker.

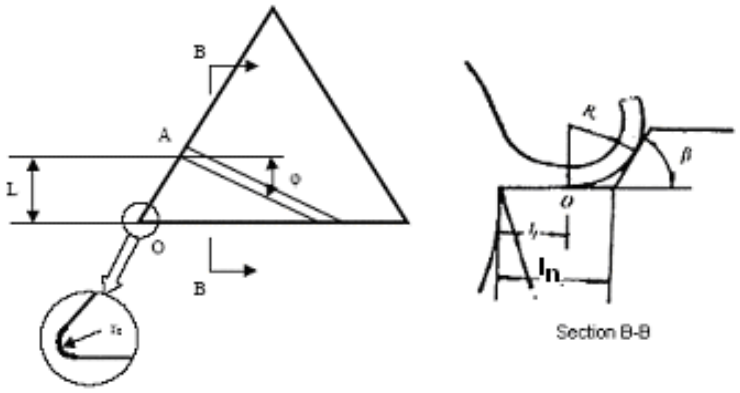

Figure 6-1 Illustration of The Geometry of The Block-Type Chip Breaker

The latest equation of chip up-curl (R_0) for block type chip-breaker was formulated by Li (1990)i.e.

$$R_0 = (l_n - l_f)\cot\frac{\beta}{2}$$

where W is rake face length, l_f is the chip/insert contact length, and β_n is the backwall angle in normal direction. In the above equation when the backwall length (l_b) is shorter than l_n, the chip will curl on backwall end.

However a new equation of R_0 established for this and future research is:

$$R_0 = \frac{h}{2}\sin\beta + (l_n - l_f)\left(\frac{(l_n - l_f)}{2h}\sin\beta + \cos\beta\right)$$

where h is backwall height. This Equation is functional when the following condition is fulfilled:

$$\sin\beta > \frac{h}{(l_n - l_f)}$$

Base on these equations of R_0 in 2-D, the 3-D equation can be formulated in the direction of side flow angle. The chip-breaking predictive model can be extracted from these theoretical equations in a similar manner to steps taken in this thesis for groove type chip breakers.

6.2.2 Inserts with Complicated Geometric Modifications

For inserts with complicated geometric modifications, the insert can be analyzed exactly like an insert with a protruded type groove. It means the insert parameters should be decomposed so that the groove is considered as a die that forms the chip; the nose radius and insert/chip restricted the contact length as the slot that control chip motion direction and amount.

6.2.3 Study on Ti17 Steel Chip-Breaking Chart

Titanium is a material that is commonly used within the medical, chemical and aerospace industries. It is used predominantly because of its excellent corrosion resistance and low weight-to-strength ratio. Titanium and its alloys are considered ‘difficult-to-machine’ materials due to the very rapid rates of tool wear which are observed at all but relatively slow cutting speeds, e.g., V=0.25–1.0 m/s. The other notable characteristic of Ti and its alloys is the formation of shear localized ’ or ‘saw-tooth’ chips. This chip type is distinctly different to the ‘continuous’ or ‘uniform-shear’ chip, which is formed during the machining of the majority of materials under conventional cutting conditions and breaking the chip is a big problem in industry.

Although there are many studies on chip formation of Ti steels, the chip-breaking phenomenon is not considered particularly in the academic area. Therefore chip breaking and a chip-breaking predictive model in Ti steels can be considered in future work.

Figure 6-5 shows a sample chip-breaking chart with inserts having protruded groove.

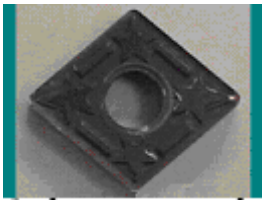

CNMG432-91 NL92 Insert

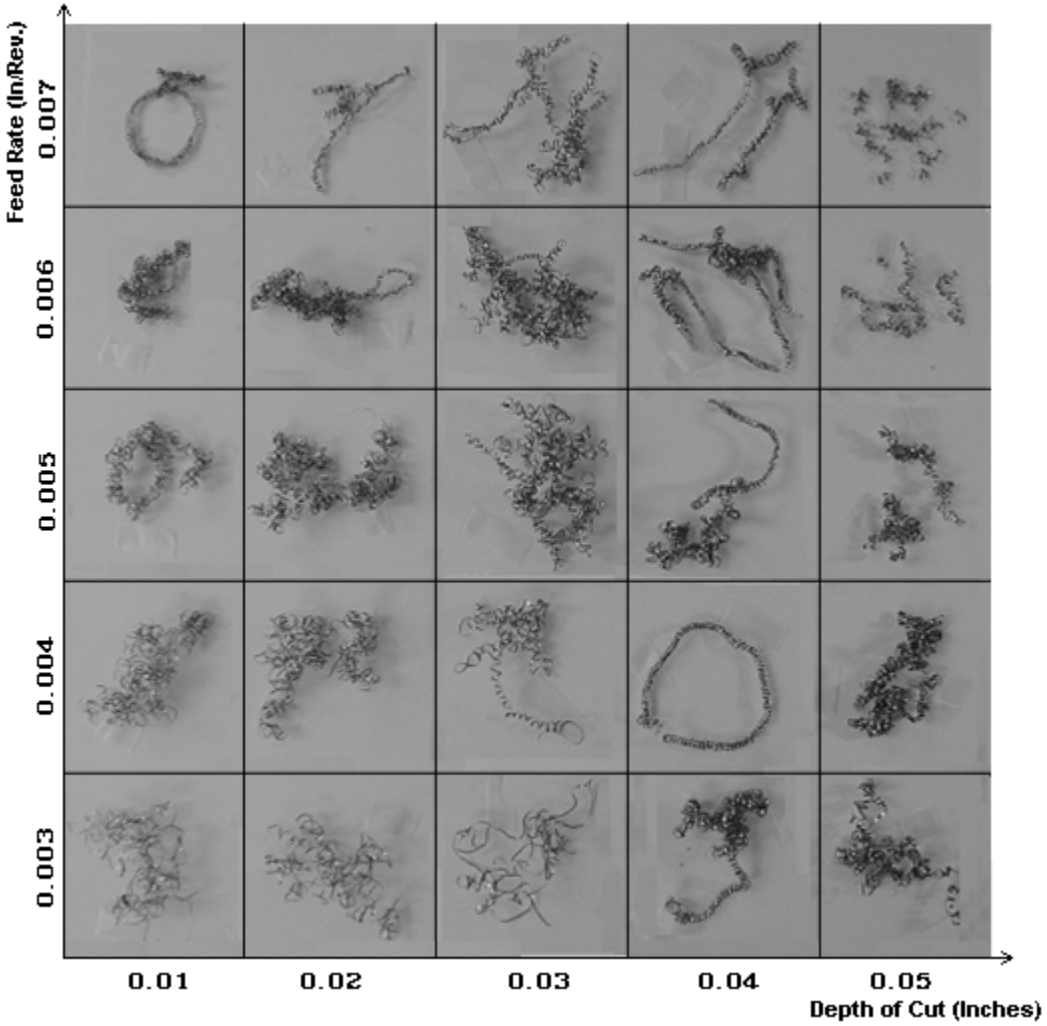

Figure 6-2 Ti17 Steel Chip-Breaking Chart

References

Bayoumi 1995
A.E. Bayoumi, J.Q. Xie, " Some Metallurgical aspects of Chip Formation in Cutting Ti-6wt.%Al-4wt.%V alloy", Material Science and Engineering A190(1995) 173-180.

Barry 2001
J. Barry , G. Byrne, D. Lennon, "Observations on chip formation and acoustic emission in machining Ti–6Al–4V alloy", International Journal of Machine Tools & Manufacture 41 (2001) 1055–1070

Brown 1983
C. A. Brown. "Material Behaviour During Chip Formation", Diss. Abstr. Int. 44(4), University of Vermont, October 1983, p.186.

Chen 1993
Y. Chen and H. Shi, "Curling and Flowing of 3-D Chips", *Journal of Huazhong University of Science and Technology,* Vol.21, No.4, 1993, pp.1-6.

Cowell 1954
L. V. Cowell, "Predicting the Angle of Chip Flow for Single Point Cutting Tools", *Transactions of ASME,* Vol.76. No.2, 1954, pp.199-202.

Dewhurst 1979
P. Dewhurst. "The Effect of Chip Breaker Constraints on the Mechanics of the Machining Process", *Annals of the CIRP,* 1979, 28 (1), pp.1-5.

Dolinšeki 2000
S. Dolinšeki, S. Ekinović, "A Contribution to The Strain-Hardening Process Analysis of Hardened Steel During High-Speed Machining"

Fang, N. 1994
N. Fang. "The Study of New-type Chip-breaking Groove Geometry of Indexable Cemented Carbide Inserts and Related CAD Technology", PhD thesis, Huazhong University of Science and Technology, Wuhan, People's Republic of China, 1994.

Fang, N. 1997
N. Fang, M. Wang, and C. Nedess. "Development of the New-type Indexable Inserts with Helical Rake Faces." *Proc. Instn Mech. Engrs*, *Part B, Journal of Engineering Manufacture*, 1997, 211(Bl), pp.159—164.

Fang, N. 2000
N. Fang. "An Auxiliary Approach to the Experimental Study on Chip Control: a Kinematically Simulated Test", *Proc Inst. Mech Engrs*, 2000, Vol 212, pp.159-166

Fang, N. 2001
N. Fang. “Kinematic Characterization of Chip Lateral-Curl - The Third Pattern of Chip Curl in Machining. ASME Journal of Manufacturing Science and Technology, In press.

Fang, N. 2001
N. Fang, I. S. Jawahir, P. L. B. Oxley. “A Universal Slip-line Model with Non-unique Solutions for Machining with Curled Chip Formation and a Restricted Contact Tool”, *International Journal of Mechanical Sciences*, 43, 2001, pp.570-580

Fang, X. 1990-a
X. D. Fang and I. S. Jawahir. “An Expert System Based on A Fuzzy Mathematical Model for Chip Breakability Assessments in Automated Machining”, *ASME Proc. Int. Conf. MI'90,* Atlanta, Georgia, USA, Vol.4, March 1990, pp.31-37.

Fang, X. 1990-b
X. D. Fang and Y. Yao. “Expert System-Supported On-line Tool Wear Monitoring”, *Proc. of International Conference on Artificial Intelligence in Engineering - AIE'90,* Sponsored by I.E.E. (UK), August 21-22, 1990, Kuala Lumpur, Malaysia, pp.77-84.

Fang, X. 1991
X. D. Fang and I. S. Jawahir, "On Predicting Chip Breakability in Machining of Steels with Carbide Tool Inserts Having Complex Chip Groove Geometries", *Journal of Materials Processing Technology (USA),* Vol.28(2), 1991, pp.37-48.

Fang, X. 1993
X. D. Fang and I. S. Jawahir, "The Effects of Progressive Tool-wear and Tool Restricted Contact on Chip Breakability in Machining", *Wear,* Vol.160, 1993, pp.243-252.

Fang, X. 1994-a
X. D. Fang and I. S. Jawahir, "Predicting Total Machining Performance in Finish Turning Using Integrated Fuzzy-Set Models of the Machinability Parameters", *International Journal of Production Research,* Vol.32(4), 1994, pp.833-849.

Fang, X. 1994-b
X. D. Fang, "Experimental Investigation of Overall Machining Performance with Overall Progressive Tool Wear at Different Tool Faces", *Wear,* Vol.173, 1994, pp.171-178.

Jawahir 1988-a
I. S. Jawahir and P. L. B. Oxley. “New Developments in Chip Control Research: Moving Towards Chip Breakability Predictions for Unmanned Manufacture”, *Proc. Int Conf ASME,* MI’88, Atlanta, Georgia, USA, April 1988, pp.311-320.

Jawahir 1988-b
I. S. Jawahir and P.L.B. Oxley, "Efficient Chip Control at Reduced Power Consumption: An Experimental Analysis", *Proceedings of the 4th International Conference on Manufacturing Engineering,* Brisbane, Australia, May 1988.

Jawahir 1988-c
I. S. Jawahir, "A Survey and Future Predictions for the Use of Chip-breaking in Unmanned Systems", *International Journal of Advanced Manufacturing Technology*, 1988, 3(4), pp.87-104.

Jawahir 1988-d
I. S. Jawahir, "The Chip Control Factor in Machinability Assessments: Recent Trends", *Journal of Mechanical Working Technology,* Vol.17, 1988, pp.213-224.

Jawahir 1988-e
I. S. Jawahir, "The Tool Restricted Contact Effect as a Major Influencing Factor in Chip-breaking", *Annals of the CIRP,* Vol.37, 1988, pp.121-126.

Jawahir 1989
I. S. Jawahir and X D. Fang. "A Knowledge-based Approach for Improved Performance with Grooved Chip Breakers in Metal Machining", *Proc. 3rd International Conference on Advances in Manufacturing Technology,* Organized by *IProdE,* Singapore, August 14-16, 1989, pp.130-144.

Jawahir 1990-a
I. S. Jawahir and X. D. Fang. "Some Guidelines on the Use of a Predictive Expert System for Chip Control in Automated Process Planning", *Proc. Fifth International Conference on Manufacturing Engineering,* Vol.1, Wollongong, Australia, July 11-13, 1990, pp.288-292.

Jawahir 1990-b
I. S. Jawahir, "On the Controllability of Chip-breaking Cycles and Modes of Chip-breaking in Metal Machining", *Annals of the CIRP,* Vol.39, 1990, pp.47-51.

Jawahir 1991
I. S. Jawahir, "An Investigation of Three-dimensional Chip Flow in Machining of Steels with Grooved Chip Forming Tool Insert", *Transactions of NAMRC*, 1991*,* 19, pp.222-231.

Jawahir 1993-a
I. S. Jawahir and C. A. van Luttervelt, "Recent Developments in Chip Control Research and Applications", *Annals of the CIRP,* 42(2)*,* 1993, pp.659-685.

Jawahir 1993-b
I. S. Jawahir, "Chip Control Literature Database", Technical Report, *Annals of the CIRP,* 42(2), 1993, pp.686-693.

Jiang 1984
C. Y. Jiang, Y. Z. Zhang and Z. J. Chi, "Experimental Research of the Chip Flow Direction and its Application to the Chip Control", *Annals of the CIRP,* Vol.33, 1984, pp.81-84.

Johnson 1970
W. Johnson, R. Sowerby and J. B. Haddow, *Plane - Strain Slip-line Fields: Theory and Bibliography.* Edward Arnold (Publishers) Ltd., London, 1970.

Kiamecki 1973
B. E. Kiamecki, "Incipient Chip Formation in Metal Cutting - A Three Dimension Finite Element Analysis", Ph.D. Dissertation, University of Illinois at Urbana-Champaign, 1973.

Kluft 1979
W. Kluft, W. Konig, C.A. van Luttervelt, K. Nakayama and A.J. Pekeiharing, "Present knowledge of chip control", *Annals of the CIRP,* Keynote Paper, 28(2), 1979, pp.441-455.

Komanduri 1982
R. Komanduri, Some clarifications on the mechanisms of chip formation when machining titanium alloys, Wear 76 (1982) 15–34.

Lajczok 1980
M. R. Lajczok, "A study of Some Aspects of Metal Machining Using Finite Element Method", Ph.D. Dissertation, N.C. State University, 1980.

Lee 1951
E. H. Lee and B.W. Shaffer, "The Theory of Plasticity Applied to a Problem of Machining", *Journal of Applied Mechanics,* Vol.73, 1951, pp.405.

Li, 1990
Z. Li, *Machining Chip-breaking Mechanism with Applications,* Dalian University press, Dalian, China, 1990 (in Chinese).

Li, 1995
Z. Li and Y. Rong, "Analysis on Formation and Breaking of C-type Side-curling chips", *Computer-aided Tooling,* ASME IMECE, San Francisco, CA, Nov. 12-I 7, 1995, MED-Vol. 2-1, pp.715-722.

Li, 1996
Z. Li, *Machining Chip-breaking Process Analysis,* Mechanical Industry Press, Beijing, China, 1996 (in Chinese).

Li, 1997
Z. Li andY. Rong, "Study on Formation and Breaking of Side-curl Screw Chips", ASME IMECE, Dallas, TX, Nov. 16-21, 1997.

Li, 1999
Z. Li andY. Rong, "A Study on Chip-breaking Limits in Machining", *Machining Science and Technology,* 3(1), 1999, pp.25-48

Lutov 1962
V. M. Lutov. “Selecting the Optimum Size of Chip-breaking Grooves”, *Machines and Tooling* 33 (7),1962, pp.27-30.

Merchant 1944
M. E. Merchant. "Basic Mechanics of the Metal Cutting Process", *Journal of Applied Mechanics,* Vol.11, 1944, p. A-168.

Merchant 1945
M. E. Merchant. "Mechanics of the Metal Cutting Process", *Journal of Applied* Physics, Vol.16, No.5, 1945, p.267.

Nakamura 1982
S. Nakamura, G. I. Wuebbling and J. D. Christopher. “Chip Control in Turning”, *Proc. Int. Tool and Manuf Eng. Conf* , SME. USA, May 1982, pp.159-177.

Nakayama 1958
K. Nakayama, "Studies of the Mechanism in Metal Cutting", *Bulletin of Faculty of Engineering,* Yokohama National University, Vol.7, 1958, p.1.

Nakayama 1962-a
K. Nakayama, "A Study on Chip-breaker”, *Bulletin of Japanese Society of Mechanical Engineers,* Vol.5, No.17, 1962, pp.142-150.

Nakayama 1962-b
K. Nakayama. “Chip Curl in Metal Cutting Process”, *Bulletin of the Faculty of Engineering; Yokohanta National Univ.,* 1962, 11, pp.1-13.

Nakayama 1963
K. Nakayama. “Pure Bending Test of Chip - An Approach to the Prediction of Cutting Force”, *Bulletin of the Faculty of Engineering. Yokohama National Univ.,* 1963, 12, pp.l-14.

Nakayama 1972-a
K. Nakayama, "Origins of Side-curl in Metal Cutting”, *Bulletin of Japanese Society of Precision Engineer)zg,* Vol.6, No.3, 1972, pp.99-101.

Nakayama 1972-b
K. Nakayama. “Origins of Side-curl of Chip in Metal Cutting”, *Bull. Japan Soc. Of Prec. Engg.,* 1972, 6(3), pp.99-101.

Nakayama 1977
K. Nakayama and M. Arai. “Roles of Brittleness of Work Material in Metal Cutting”, *Proc. Int. Symposium on Influence of Metallurgy on Machinability” of Steel.,* Sept. 1977, Tokyo. Japan. pp.421-432.

Nakayama 1978
K. Nakayama and M. Ogawa. “Basic Rules on the Form of Chip in Metal Cutting”, *Annals of the CIRP*, 27(1), 1978, pp.17-21.

Nakayama 1979
K. Nakayama, "Basic Rules on The Form of Chip in Metal Cutting", *Annals of CIRP,* Vol.28, 1979, p.17.

Nakayama 1981
K. Nakayama, "Cutting Tool with Curved Rake Face - A Means for Breaking Thin Chips", *Annals of CIRP,* Vol.30, 1981, pp.5-8.

Nakayama 1984
K. Nakayama, "Chip Control in Metal Cutting”, *Bulletin of Japanese Society of Precision Engineering,* Vol.18, No.2, 1984, pp.97-103.

Nakayama 1986
K. Nakayama, Z. Li, and M. Arai, "Performance of the Chip breaker of Cutting Tool (1st report): Range of Cutting Conditions for Chip-breaking”, *Journal of JAPE,* Vol.52, No.12, 1986, pp.126-131.

Nakayama 1990
K. Nakayama and M. Arai, "The Breakability of Chip in Metal Cutting”, *Proc. Int. Conf. On Manufacturing Engineering,* Melbourne, Australia, 1990, pp.6-10.

Okoshi 1967
M. Okoshi and K. Kawata. “Effects of the Curvature on Work Surface on Metal Cutting”, *Annals of the CIRP 15,* 1967, pp.393-403

Okushima 1959
K. Okushima, and K. Minato, “On the Behaviors of Chips in Steel Cutting”, *Bulletin JSME, 2(5),* 1959

Okushima 1960
K. Okushima, T. Hoshi, and T. Fujinawa, “On the Behaviors of Chips in Steel Cutting”, *Bulletin JSME, 3(10),* May, 1960

Oxley 1962
P. L. B. Oxley. “An Analysis for Orthogonal Cutting with Restricted Tool-Chip Contact”, *Int. J. Mech. Sci.,* 1962, 4, pp.129-135.

Oxley 1963-a
P. L. B. Oxley and M.J.M. Welsh, "Calculating the Shear Angle in Orthogonal Metal Cutting from Fundamental Stress, Strain, Strain-Rate Properties of the Work Material", *Proceedings 4th International Machine Tool Design and Research Conference,* Pergamon, Oxford, 1963, pp.73-86.

Oxley 1963-b
P. L. B. Oxley, "Mechanics of Metal Cutting", Proceedings of International Production Engineering Research Conference, Pittsburgh, 1963, p.50.

Palmer 1959
W. B. Palmer, and P.L.B. Oxley, "Mechanics of Metal Cutting", *Proceedings of the Institution of Mechanical Engineers,* Vol.173, 1959, p.623.

Rahman 1993
M. Rahman, K.H.W. Seah, X.P. Li, and X.D. Zhang, "A Three Dimensional Model of Chip Curl and Chip Breaking Under the Concept of Equivalent Parameters", International Journal of Machine Tool Manufacturing", Vol. 35, No. 7. pp.1015-1031, 1993.

Rahman 1996
M. Rahman, K.H.W. Seah, X.P. Li, and X.D. Zhang, "A Three-Dimensional Model of Chip Flow, Chip Curl and Chip Breaking for Oblique Cutting", Ins. J. Mech. Tools Manufact. VoL 36, No. 12, pp. 1385-1400, 1996

Ramalingam 1980
S. Ramalingam and P. V. Desai. "Tool-Chip Length in Orthogonal Machining", *ASME* Paper 80, WA/Prod. 23, 1980.

Shaw 1953
M. C. Shaw, N.H. Cook, and I. Finnie, "The Shear-Angle Relationship in Metal Cutting", *Transaction ASME,* Vol.75, 1953, pp.273-283.

Shaw 1963
M. C. Shaw. "Resume and Critique of Papers in Part One", *Proc. Int. Prod. Eng. Res. Conf. ASME.* Pittsburgh, September 1963, pp.3-17.

Shaw 1984
M. C. Shaw, *Metal Cutting Principles,* Oxford Series on Advanced Manufacturing, 1984.

Shinozukza 1996
J. Shinozukza. "Chip Breaking Analysis from the Viewpoint of the Optimum Cutting Tool Geometry Design". Journal of Materials Processing Technology. 62(1996) 345-351.

Shivathaya 1993
S. Shivathaya and X. D. Fang. "Hybrid Knowledge-Based Tool Room Scheduling", *Proc. Australian Conference on Manufacturing Engineering,* Adelaide, Australia, Nov., 1993, pp.215-222.

Shivathaya 1994
S. Shivathaya, X. D. Fang and J.G. Williams. "Knowledge Elicitation for Material Design Expert System", *9th International Conf. of AIENG'94 (Application of Artificial Intelligence in Engineering),* 19-21 July 1994, Philadelphia, U.S.A., pp.117-124.

Spaans 1970-a
C. Spaans and P. F. H. J. van Geel, "Breaking Mechanisms in Cutting with a Chip Breaker", *Annals of the CIRP,* Vol. 18, 1970, pp.87-92.

Spaans 1970-b
C. Spaans. "A Systematic Approach to Three Dimensional Chip Curl, Chip-breaking and Chip Control", SME Paper 7-241, 1970.

Spaans 1971-a
C. Spaans. "A Comparison of an Ultrasonic Method to Determine the Chip/Tool Contact Length with Some Other Methods", *Annals of the CIRP* 19, 1971, pp.485-490.

Spaans 1971-b
C. Spaans. "The Fundamentals of Three-Dimensional Chip Curl, Chip-breaking and Chip Control", Doctoral Thesis, TH Delft, 1971.

Stabler 1951
V. G. Stabler, "The Fundamental Geometry of Cutting Tool", *Proc. Inst. Mech. Engg.,* 165, 1951.

Stabler 1964
V. G. Stabler, "The Chip Flow Law and its Consequence", *Proc.* 5th *International Machine Tool Design and Research Conference,* Birmingham, UK, 1964, pp.243-251.

Strenkowski 1985
J. S. Strenkowski and J.T. Carroll, "A Finite Element Model of Orthogonal Metal Cutting", *Journal of Engineering for Industry,* Vol.107, 1985, p.346.

Strenkowski 1990
J. S. Strenkowski and K.J. Moon, "Finite Element Prediction of Chip Geometry and Tool/Workpiece Temperature Distribution in Orthogonal Cutting", *Journal of Engineering for Industry,* Vol.112, 1990, pp.313-318.

Tolouei 1993-a
M. Tolouei Rad and X.D. Fang. "Application of Expert Systems in Design of Deep-Drawing Dies for Circular Shells", *Proc. Production and Manufacturing Engineering Conference (PMEC),* Tehran, fran, Oct., 1993, pp.143-151.

Tolouei 1993-b
M. Tolouei Rad and X.D. Fang. "Artificial Intelligence-based Design of Deep-Drawing Pressing Dies", *Proc. Australian Conference on Manufacturing Engineering,* Adelaide, Australia, Nov., 1993, pp.267-272.

Usui 1962
E. Usui and M.C. Shaw, "Free Machining Steel-IV, Tool with Reduced Contact Length", *Journal of Engineering for Industry,* Vol.84, 1962, p.89.

Usui 1963
E. Usui and K. Roshi, "Slip-line fields in metal machining which involve centered fans", *Proceedings of International Production Engineering Research* (ASME Conference), Pittsburgh, September 1963, pp.61-71.

Usui 1964
E. Usui, K. Kikuchi and R. Hoshi, "The theory of plasticity applied to machining with cut-away tools", *Transactions ASME, Journal of the Engineering Industry*, May 1964, pp.95-104.

Van Luttervelt 1976
C. A. van Luttervelt. “Chip Formation in Machining Operation at Small Diameter”, *Annals of the CIRP 25(I),* 1976, pp.7l-76

Van Luttervelt 1989
C. A. van Luttervelt, "Evaluation of present possibilities of chip control", *VDI Berichte* 762, 1989, pp.181-200.

Von Turkovich 1981
B. F. von Turkovich, "Metallurgy – A Foundation for Understanding the Art of Machining", *Proc. Winter Annual Meeting of ASME*, Washington D. C., 1981, PED-Vol .3.

Wallace 1968
P. W. Wallace and G. Boothroyd, "Tool Forces and Tool-Chip Friction in Orthogonal Cutting", *Journal of Engineering for Industry,* Vol.90, 1968, pp.54-62.

Worthington 1979
B. Worthington and M. H. Rahman, "Prediction Breaking with Groove type Breakers”, *International Journal of Machine Tool Design and Research,* Vol. 19, 1979, pp.121-132.

Wright 1977
P. K. Wright. “Applications of the Experimental Methods used to Determine Temperature Gradients in Cutting Tools”, *Proc. Australian Conf. on Manuf. Engineering.,* Aug. 1977, pp.145-149.

Young 1987
H. T. Young, P. Mathew and P.L.B. Oxley, "Allowing for nose radius effects in predicting the chip flow direction and cutting forces in bar turning", *Proceedings of the Institute of Mechanical Engineers* 201(C3), 1987, pp.213-226.

Zhang 1980
Y. Z. Zhang, "Chip Curl, Chip-breaking, and Chip Control of the Difficult-to-cut Materials”, *Annals of the CIRP,* Vol.29, 1980, pp.79-83.

Zhang 1993-a
Y. Zhang and X. D. Fang. "Minimizing the Number of Surplus Components in Selective Assembly via a Fuzzy-set Model", *Proc. 12th International Conf on Assembly Automation,* Adelalde, Australia, Nov.1993, pp.61-67.

Zhang 1993-b
Y. Zhang and X.D. Fang. "A New Method for Sampling Inspection by Variables under Undesired Measurement Conditions", *Proc. 2nd International Symposium on Measurement Technology and Intelligent Instrument,* Wuhan, China, Oct., 1993, pp.74-83.

Zhou 2001-a
L. Zhou, H. Guo and Y. Rong, "Machining Chip Breaking Prediction", *4th Inernational Machining & Grinding Conference, of SME,* SME paper 601, Troy, Michigan, May 7-10, 2001.

Zhou 2001-b
Zhou Li "Machining Chip-Breaking Prediction with Grooved Inserts in Steel Turning", Ph.D. Research dissertation, 2001

APPENDIX A. Measured Side Flow Angles

Side Flow Angles measured in AutoCAD Software In shown depth of cut and feed rate by CNMG432-NL92 Insert.

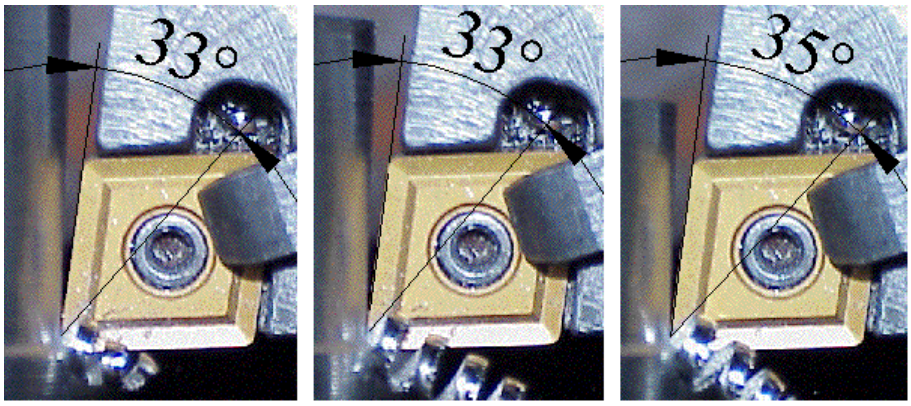

Figure A-1 Depth of Cut 0.03 in. Feed Rate 0.011 in/rev

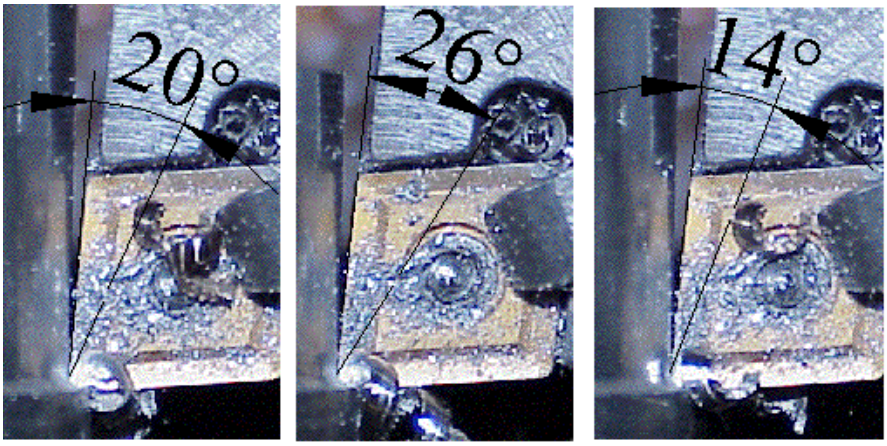

Figure A-2 Depth of Cut 0.05 in. Feed Rate 0.011 in/rev

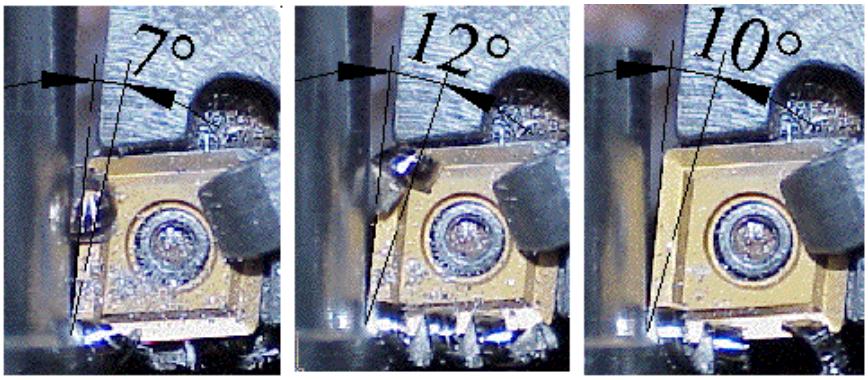

Figure A-3 Depth of Cut 0.06 in. Feed Rate 0.011 in/rev

APPENDIX B. Measured Chips

The following pictures are the measured chips produced by CNMG432-NL92 insert in AutoCAD software. The material of chips is 4150 steel and measurements unit are inches

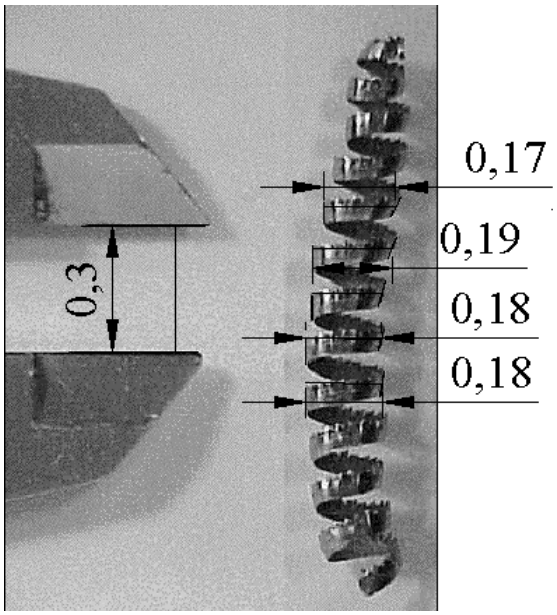

Figure B-1 Chip Dimensions Produced by 0.03 in. Depth of Cut and 0.011 in/rev Feed Rate

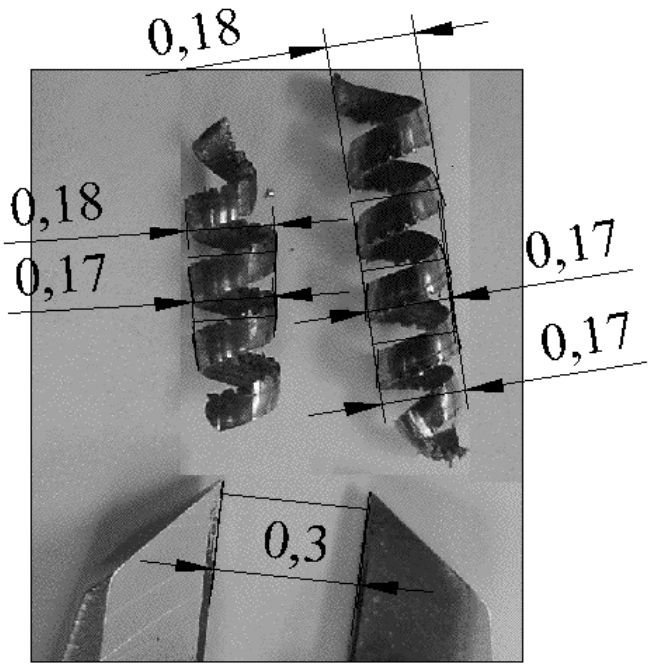

Figure B-2 Chip Dimensions Produced by 0.05 in. Depth of Cut and 0.011 in/rev Feed Rate

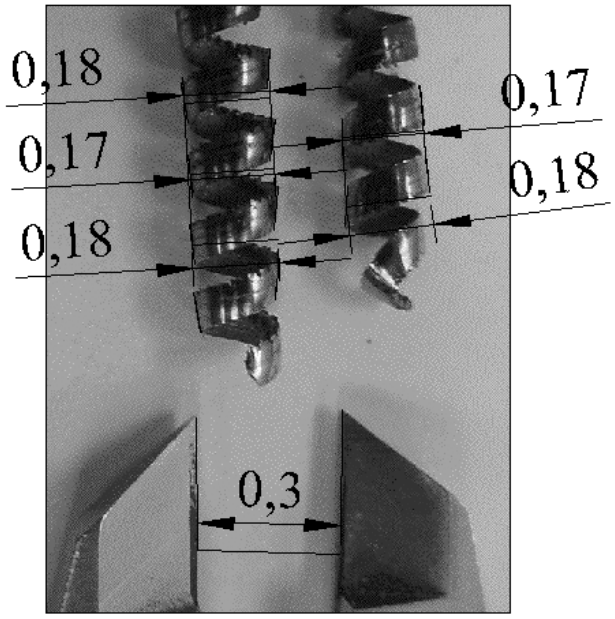

Figure B-3 Chip Dimensions Produced by 0.06 in. Depth of Cut and 0.011 in/rev Feed Rate

APPENDIX C. Chip-Breaking Charts of Protruded Groove Inserts

The chip-breaking charts shown next are from the study on chip-breaking limits of three-dimensional grooved inserts. The workpiece material used in the tests was 1010 steel. The surface speed was V_C = 523 sfpm.

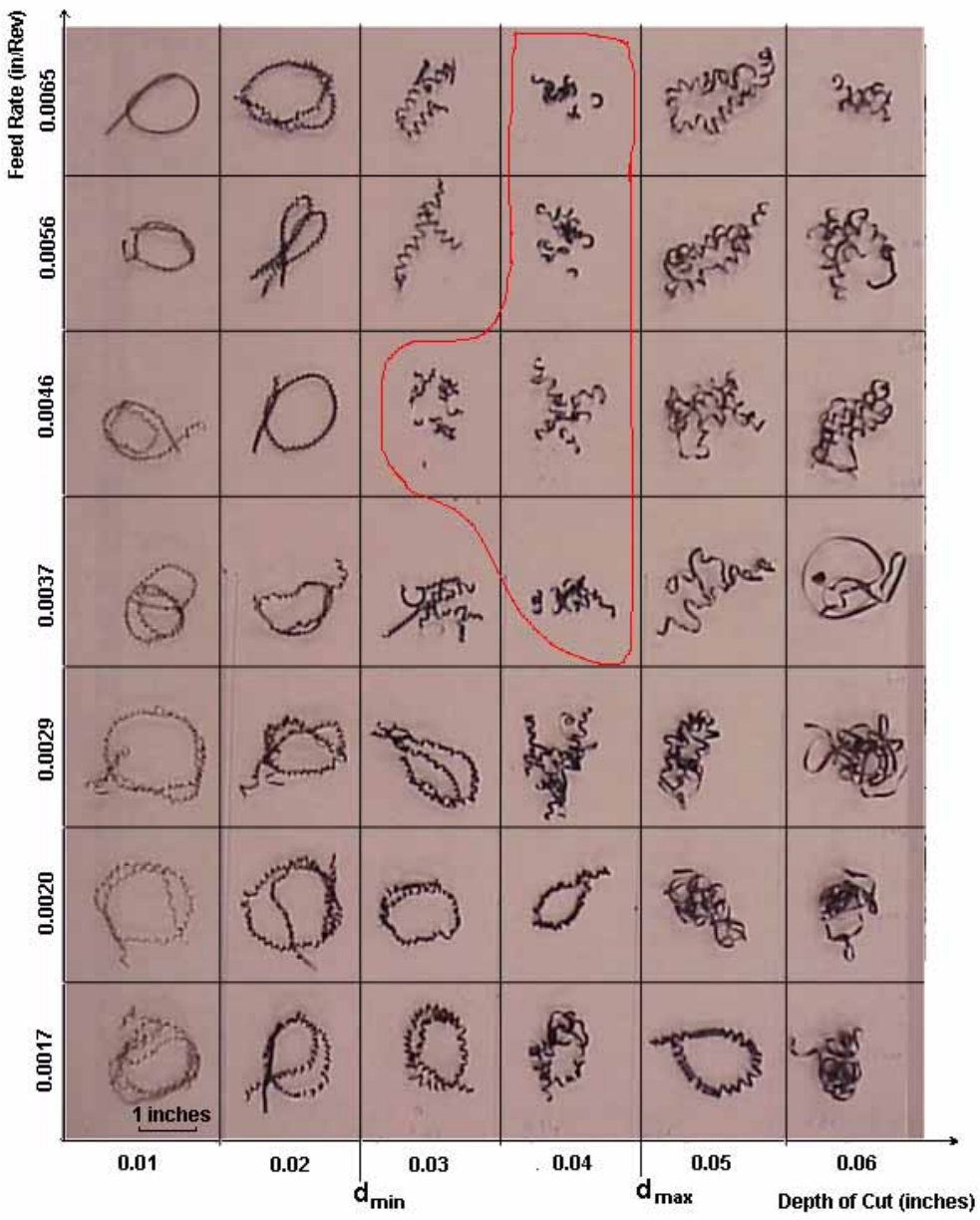

Figure C-1 TNMG QF 333 4025 Insert Chip-Breaking Chart

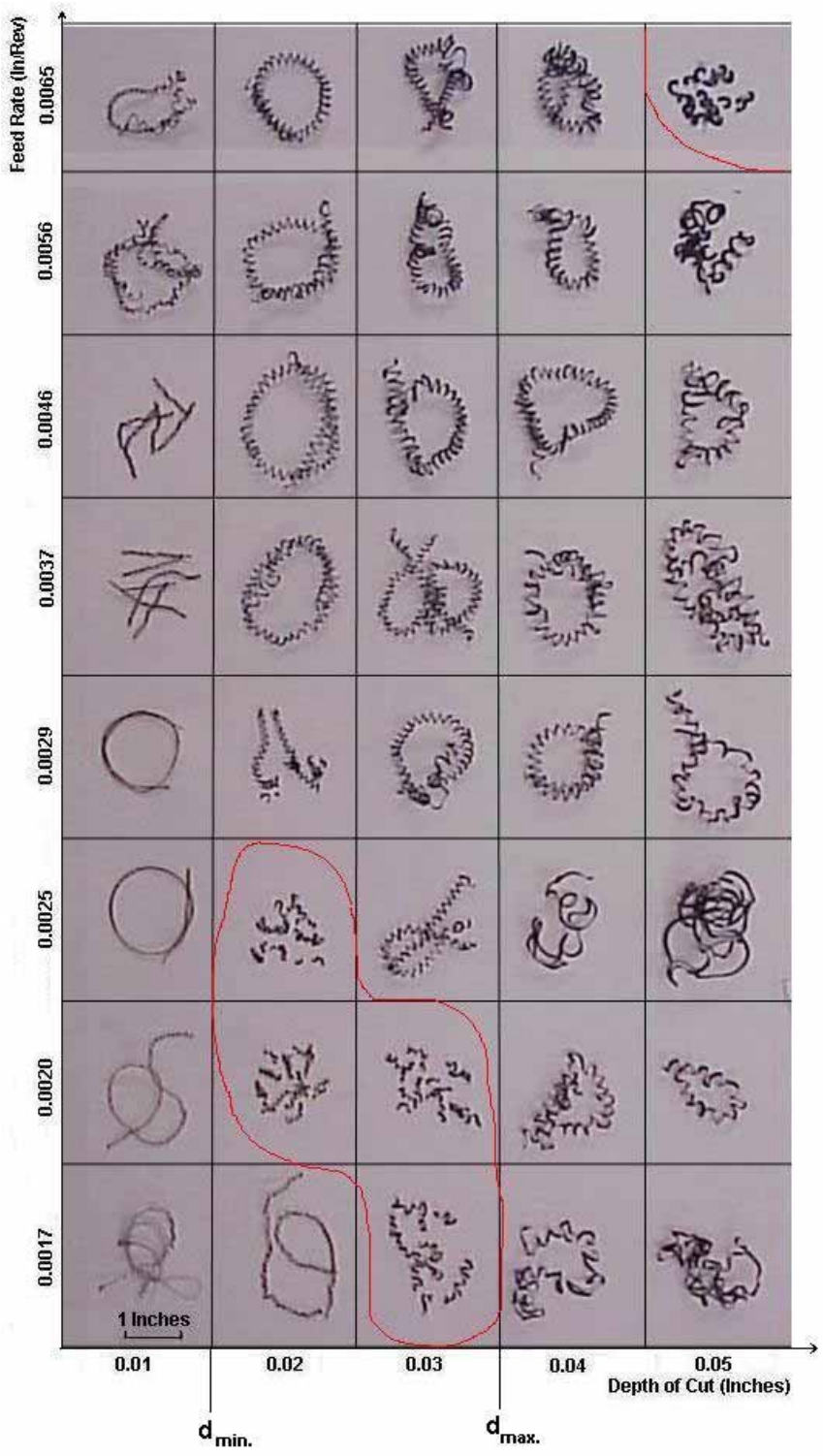

Figure C-2 TNMG QF 332 4025 Insert Chip-Breaking Chart

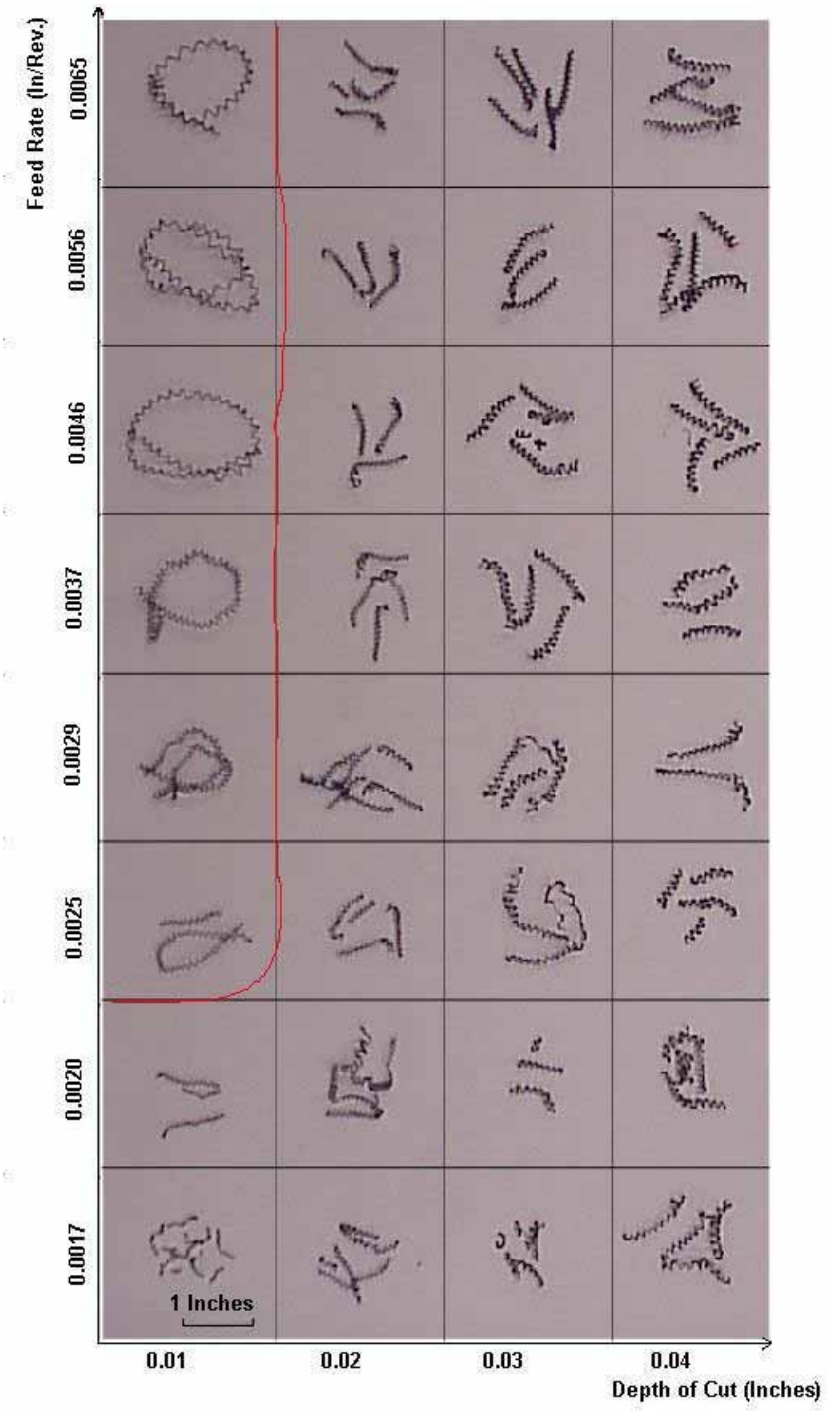

Figure C-3 TNMG QF 332 4025 Insert Chip-Breaking Chart

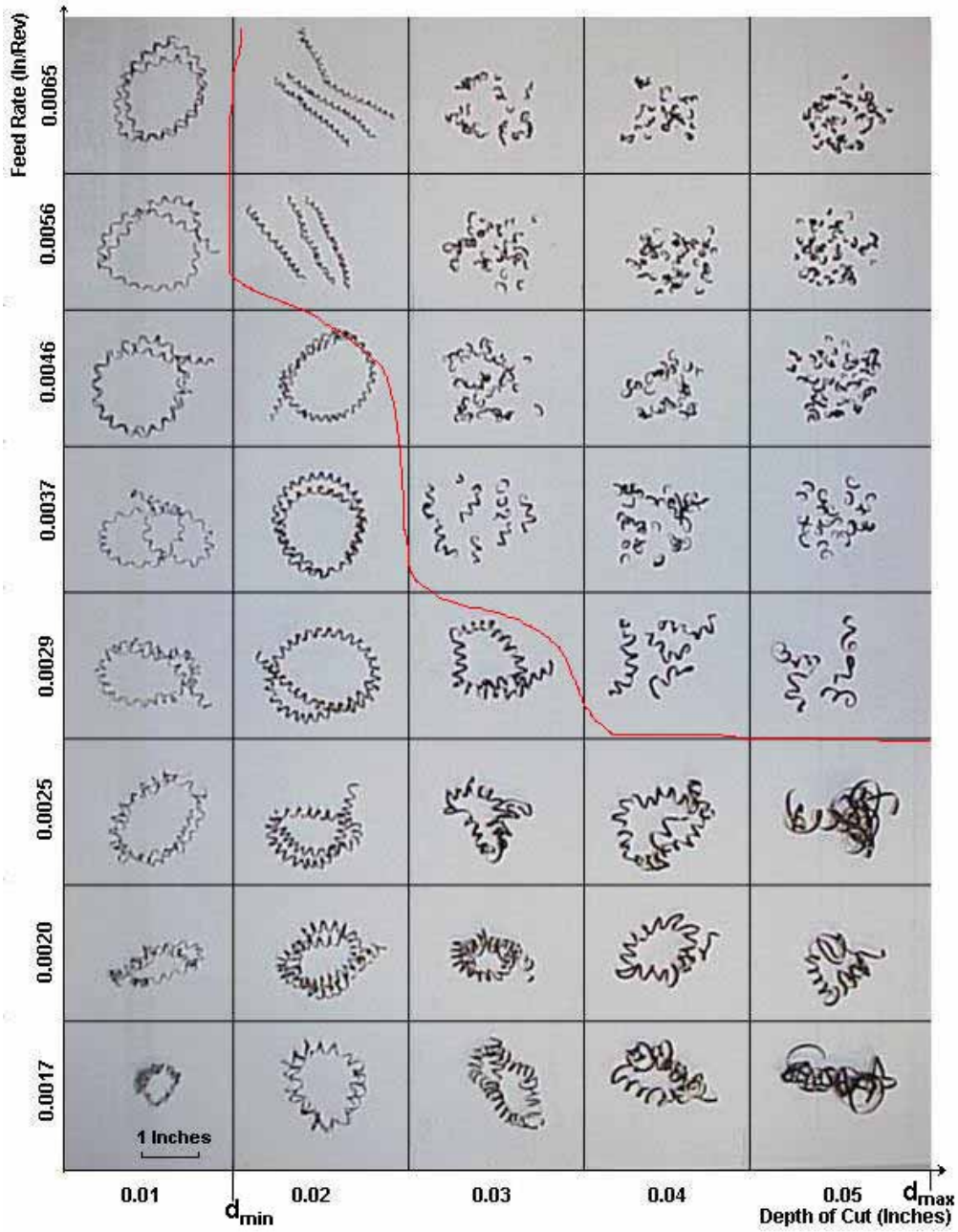

Figure C-4 TNMG 332K KC850 Insert Chip-Breaking Chart